

INVERSE REGRESSION FOR RIDGE RECOVERY: A DATA-DRIVEN APPROACH FOR PARAMETER SPACE DIMENSION REDUCTION IN COMPUTATIONAL SCIENCE*

ANDREW GLAWS[†], PAUL G. CONSTANTINE[‡], AND R. DENNIS COOK[§]

Abstract. Parameter space dimension reduction can enable otherwise infeasible design and uncertainty studies with modern computational science models that contain several input parameters. In statistical regression, techniques for *sufficient dimension reduction* (SDR) use data to reduce the predictor dimension of a regression problem. A computational scientist hoping to use SDR for parameter space dimension reduction encounters a problem: a computer prediction is best represented by a deterministic function of the inputs, so data comprised of computer simulation queries fail to satisfy the SDR assumptions. To address this problem, we interpret SDR methods *sliced inverse regression* (SIR) and *sliced average variance estimation* (SAVE) as estimating the directions of a *ridge function*, which is a composition of a low-dimensional linear transformation with a nonlinear function. Within this interpretation, SIR and SAVE estimate matrices of integrals whose column spaces are contained in the ridge directions' span; we analyze and numerically verify convergence of these column spaces as the number of samples increases. Moreover, we show example functions that are not ridge functions but whose inverse conditional moment matrices are low-rank. Consequently, the computational scientist should beware when using SIR and SAVE for parameter space dimension reduction, since SIR and SAVE may mistakenly suggest that truly important directions are unimportant.

Key words. sufficient dimension reduction, ridge functions, ridge recovery

AMS subject classifications. 62B99, 65C60, 65C05

1. Introduction and related literature. Data science and machine learning methods are essential tools in modern data-driven computational science and engineering. The computational scientist frequently uses supervised learning techniques (i.e., curve fitting) to identify trends, quantify uncertainty, predict unobserved phenomena, and optimize engineered designs in complex physical systems. The most commonly used supervised learning approaches include methods for regression modeling (as opposed to classification), since both input features and output quantities of interest are best modeled as continuous real variables. These approaches appear under several names: response surfaces [42, 34], surrogate models [47, 3], metamodels [55], and emulators [4]; we use the term *response surface* in the remainder.

We generically model a physics-based input/output system as a function $f(\mathbf{x})$, where \mathbf{x} represents a vector of continuous physical inputs and f represents a continuous physical output of interest. It is common to treat f as a deterministic function, since a bug-free computational model produces the same outputs given the same inputs; in other words, there is no random noise in simulation outputs. This perspective

*Submitted to the editors DATE.

Funding: The first author's work was supported by the Ben L. Fryrear Ph.D. Fellowship in Computational Science and the DARPA DSO Enabling Quantification of Uncertainty in Physical Systems program. The second author's work was supported by the DARPA DSO Enabling Quantification of Uncertainty in Physical Systems program and the U.S. Department of Energy Office of Science, Office of Advanced Scientific Computing Research, Applied Mathematics program under Award Number DE-SC-0011077.

[†]Department of Computer Science, University of Colorado, Boulder, CO (andrew.glaws@colorado.edu).

[‡]Department of Computer Science, University of Colorado, Boulder, CO (paul.constantine@colorado.edu).

[§]Department of Applied Statistics, University of Minnesota, St. Paul, MN (dennis@stat.umn.edu, <http://users.stat.umn.edu/~rdcook/>).

is the de facto setup in the statistics subfield of *computer experiments* [48, 35, 49], where Gaussian process regression [46] is the supervised learning tool of choice. The setup is similar in the field of *uncertainty quantification* [50, 52, 26]; although the inputs may be modeled as random variables to represent aleatory uncertainty, the input/output map is deterministic.

Several important, oft overlooked mathematical challenges arise when applying regression methods to a dataset comprised of point queries of a deterministic function. In regression modeling [56], the given data are predictor/response pairs $\{(\mathbf{x}_i, y_i)\}$ that are assumed to be independent realizations of a random vector with a joint predictor/response probability density function. If the response is a deterministic function of the predictors, then such a density cannot exist. Thus, the data from computational science simulations fail to satisfy the regression assumptions. This failure has important consequences for interpreting *error* and *convergence* in the response surface. We do not explore these consequences in this paper, but the differences between statistical regression and function approximation are essential to our thesis.

Nonparametric regression approaches are most appropriate for computational science data since the physical complexities produce nonlinear responses. However, the nonlinearity implies that response surface construction suffers from the *curse of dimensionality* [20, 53]; loosely, the number of function queries needed to construct an accurate response surface grows exponentially with the input predictor dimension. In computational science, this curse is exacerbated by the computational cost of each query, which often involves the numerical approximation of a system of partial differential equations. In high dimensions (i.e., several physical input parameters), the number of queries needed to reach error estimate asymptopia (or even construct the response surface) is generally considered infeasible. The computational scientist may attempt to simplify the model by fixing unimportant input parameters at nominal values, thus reducing the dimension of the input space to the point that response surface modeling becomes practical.

Both linear [19] and nonlinear [36] dimension reduction methods are well known in unsupervised learning, and they are appropriate for computational science input parameter spaces when there is a relationship (e.g., correlation structure) among the input parameters. However, in many cases the physical inputs are independent. Therefore we must use dimension reduction approaches, such as active subspaces [7], that are derived from low-dimensional structure in the input/output map.

In regression modeling, subspace-based predictor space dimension reduction goes by the name *sufficient dimension reduction* (SDR) [14, 2]. Techniques for SDR include sliced inverse regression (SIR) [37], sliced average variance estimation (SAVE) [17], ordinary least squares (OLS) [39], and principal Hessian directions (pHd) [38]—among several others. These techniques seek a low-dimensional subspace in the predictor space that is sufficient to statistically characterize the relationship between predictors and response. Related techniques and extensions have enabled feature space dimension reduction in supervised learning models [41, 58, 25]. And SDR methods are gaining interest for parameter space dimension reduction in computational science [40, 60, 43]. The first use we know applies OLS, SIR, and pHd to a contaminant transport model from Los Alamos National Labs, where the results revealed simple, exploitable relationships between transformed inputs and the computational model’s output [12, Section 4]. However, these papers do not carefully address the important mathematical differences that arise when applying a technique developed for statistical regression to study a deterministic function. A data set comprised of point queries from a deterministic function (e.g., an experimental design in the physical inputs and

associated computer model predictions) differs from the regression data set (independent draws of a joint predictor/response distribution). How does one interpret a dimension reduction subspace from SIR or SAVE when there is no random noise in the functional relationship between inputs and outputs? What does *sufficient dimension reduction* mean for deterministic functions?

We evaluate and analyze the *inverse regression* methods SIR and SAVE as candidates for gradient-free subspace-based input space dimension reduction in deterministic functions. SIR- and SAVE-style dimension reduction follows from low-rank structure in the regression’s inverse conditional moment matrices. The appropriate way to interpret SIR and SAVE in this context is as methods for *ridge recovery*. A function of several variables is a *ridge function* when it is a composition of a low-dimensional linear transformation with a nonlinear function of the transformed variables [44]—i.e., $f(\mathbf{x}) = g(\mathbf{A}^\top \mathbf{x})$ where \mathbf{A} is a tall matrix. The goal of ridge recovery is to estimate the matrix \mathbf{A} (more precisely, \mathbf{A} ’s column space known as the *ridge subspace*) using only point queries of f . Recent work by Fornasier, Schnass, and Vybiral [23] and related work by Tyagi and Cevher [54] develop ridge recovery algorithms that exploit a connection between a linear measurement of a gradient vector and the function’s directional derivative to estimate \mathbf{A} with finite differences. Constantine, Eftekhari, and Wakin [10] exploit a similar connection to estimate active subspaces with directional finite differences. In contrast, the inverse regression approach for ridge recovery is based on conditional moments of the predictors given the response; we detail how this difference (gradients versus inverse conditional moments) affects the methods’ ability to recover the ridge directions.

1.1. Main results and discussion. We develop and interpret sufficient dimension reduction theory in the context of input space dimension reduction for a deterministic scalar-valued function of several variables. By this interpretation, SDR methods translate naturally as ridge recovery methods; loosely, the noiseless analog of SDR is ridge recovery. This interpretation illuminates the theoretical limitations of inverse regression for parameter space dimension reduction. We show that, if the data-generating function is a ridge function, then the population (i.e., no error from finite sampling) SIR and SAVE subspaces are (possibly strict) subspaces of the function’s ridge subspace. Consequently, the rank of the inverse conditional moment matrices is bounded above by the dimension of the ridge subspace. We also show how the inverse conditional moments become integrals, so that the finite-sample SIR and SAVE algorithms can be viewed as numerical integration methods. By choosing input samples independently at random, SIR and SAVE become Monte Carlo methods; we analyze the convergence of SIR and SAVE subspaces as the number N of samples increases and derive the expected $\mathcal{O}_p(N^{-1/2})$ rate, where \mathcal{O}_p denotes convergence in probability and the constant depends inversely on associated eigenvalue gap. Moreover, this view enables more efficient numerical integration methods than Monte Carlo for SIR and SAVE [27].

1.2. Practical considerations and scope. Some readers want to know how these results impact practice before (or in lieu of) digesting the mathematical analysis. In practice, the computational scientist does not know whether her model’s input/output map is a ridge function, and she’d like to use SIR and SAVE as a tool to test for possible dimension reduction; our theory gives some insight into this use case. First, in the idealized case of no finite-sampling (or numerical integration) error, SIR and SAVE can still mislead the practitioner, since there are non-ridge functions whose inverse conditional moment matrices are low-rank. Arguably, these may be

pathological cases that do not arise (frequently) in practice, but quantifying this argument requires mathematically characterizing a *typical problem* found in practice. We believe these failure modes should be well known and guarded against. Second, finite sample estimates (or numerical approximations) of the inverse conditional moment matrices will never have trailing eigenvalues that are exactly zero due to the finite sampling—even when the data-generating function is an exact ridge functions. This implies it may be difficult to distinguish between finite-sample noise in the eigenvalues and directions of small-but-nonzero variability in the function. The latter structure indicates anisotropic parameter dependence that is arguably more common in real world functions than exact ridge functions, and it (the anisotropy) can be exploited for ridge approximation (as opposed to ridge recovery). Because of such indistinguishability, we recommend exercising caution when using the estimated SIR and SAVE subspaces to build ridge approximations. Principally, heuristics such as bootstrapping or cross validation might help distinguish between finite sample noise and directions of relatively small variability. Third, we have found that breaking the elliptic symmetry assumption on the input density (see Section 2.1)—e.g., when the input density is uniform on a hyperrectangle—may produce nonzero eigenvalues in the inverse conditional moment matrices even when the data-generating function is an exact ridge function; distinguishing these effects from finite-sample effects or true variability in the data-generating function may be difficult. All these issues, though important in practice, are outside the scope of the present work. However, we do make some comments on practical considerations in the numerical example in Section 5.3.

1.3. Paper outline. The remainder is structured as follows. Section 2 reviews (i) the essential theory of sufficient dimension reduction in statistical regression and (ii) the SIR and SAVE algorithms. In Section 3, we review ridge functions and the ridge recovery problem. Section 4 translates SDR to deterministic ridge recovery and analyzes the convergence of the SIR and SAVE subspaces. Section 5 shows numerical examples that support the analyses using (i) two quadratic functions of ten variables and (ii) a simplified model of magnetohydrodynamics with five input parameters. Section 6 contains concluding remarks. To improve readability, all proofs are in the Appendix.

2. Sufficient dimension reduction. We review the essential theory of sufficient dimension reduction (SDR); our notation and development closely follow Cook’s *Regression Graphics: Ideas for Studying Regressions through Graphics* [14]. The theory of SDR provides a framework for subspace-based dimension reduction in statistical regression. A regression problem begins with predictor/response pairs $\{[\mathbf{x}_i^\top, y_i]\}$, $i = 1, \dots, N$, where $\mathbf{x}_i \in \mathbb{R}^m$ and $y_i \in \mathbb{R}$ denote the vector-valued predictors and scalar-valued response, respectively. These pairs are assumed to be independent realizations from the random vector $[\mathbf{x}^\top, y]$ with unknown joint probability density function $p_{\mathbf{x},y}$. The object of interest in regression is the conditional random variable $y|\mathbf{x}$; the statistician uses the given predictor/response pairs to estimate statistics of $y|\mathbf{x}$ —e.g., moments or quantiles. SDR searches for a subspace of the predictors that is sufficient to describe $y|\mathbf{x}$ with statistics derived from the given predictor/response pairs.

The basic tool of SDR is the *dimension reduction subspace* (DRS).

DEFINITION 1 (Dimension reduction subspace [13]). *Consider a random vector*

$[\mathbf{x}^\top, y]$, and let $\mathbf{A} \in \mathbb{R}^{m \times n}$ with $n \leq m$ be such that

$$(2.1) \quad y \perp\!\!\!\perp \mathbf{x} | \mathbf{A}^\top \mathbf{x},$$

where $\perp\!\!\!\perp$ denotes independence of y and \mathbf{x} . A dimension reduction subspace \mathcal{S}_{DRS} for $y|\mathbf{x}$ is

$$(2.2) \quad \mathcal{S}_{\text{DRS}} = \mathcal{S}_{\text{DRS}}(\mathbf{A}) = \text{colspan}(\mathbf{A}).$$

Equation (2.1) denotes the conditional independence of the response and predictors given $\mathbf{A}^\top \mathbf{x}$. We can define a new random variable $y|\mathbf{A}^\top \mathbf{x}$ that is the response conditioned on the n -dimensional vector $\mathbf{A}^\top \mathbf{x}$. If $\mathcal{S}_{\text{DRS}}(\mathbf{A})$ is a DRS for $y|\mathbf{x}$, then the conditional CDF for $y|\mathbf{x}$ is the conditional CDF for $y|\mathbf{A}^\top \mathbf{x}$ [14, Chapter 6]. If a regression admits a low-dimensional ($n < m$) DRS, then the predictor dimension can be reduced by considering $y|\mathbf{A}^\top \mathbf{x}$. Note that the matrix \mathbf{A} in (2.2) is not unique in defining a DRS [11]. Any matrix with the same column space is a basis for \mathcal{S}_{DRS} .

A given regression problem may admit multiple DRSs. We require a uniquely-defined DRS to ensure a well-posed SDR problem. To this end, we consider the *central dimension reduction subspace* or simply the *central subspace*.

DEFINITION 2 (Central subspace [13]). *A subspace $\mathcal{S}_{y|\mathbf{x}}$ is a central subspace for $y|\mathbf{x}$ if it is a DRS and $\mathcal{S}_{y|\mathbf{x}} \subseteq \mathcal{S}_{\text{DRS}}$, where \mathcal{S}_{DRS} is any DRS for $y|\mathbf{x}$.*

When the central subspace exists it is the intersection of all other DRSs,

$$(2.3) \quad \mathcal{S}_{y|\mathbf{x}} = \bigcap \mathcal{S}_{\text{DRS}}$$

for all \mathcal{S}_{DRS} of $y|\mathbf{x}$. The intersection in (2.3) always defines a subspace, but this subspace need not satisfy the conditional independence from Definition 1. Therefore, a regression need not admit a central subspace. However, when a central subspace exists, it is the unique DRS of minimum dimension for $y|\mathbf{x}$ [14, Chapter 6]. This minimum dimension is referred to as the *structural dimension* of $y|\mathbf{x}$.

There are a variety of conditions that ensure the existence of $\mathcal{S}_{y|\mathbf{x}}$ for a given regression problem. We consider the following condition on the marginal density $p_{\mathbf{x}}$ of the predictors.

THEOREM 2.1 ([14]). *Suppose that \mathcal{S}_1 and \mathcal{S}_2 are two DRSs for $y|\mathbf{x}$ where the marginal density of the predictors $p_{\mathbf{x}}(\mathbf{x})$ has support over a convex set. Then, $\mathcal{S}_1 \cap \mathcal{S}_2$ is also a DRS.*

According to Theorem 2.1, if $p_{\mathbf{x}}$ has support over a convex set, then any intersection of DRSs will be a DRS—i.e., $\mathcal{S}_{y|\mathbf{x}}$ from (2.3) is a DRS and (hence) the central subspace. In regression practice, this existence condition may be difficult to verify from the given predictor/response pairs. Existence of the central subspace can be proven under other sets of assumptions, including a generalization of Theorem 2.1 to M-sets [59] and another based on location regressions [14, Ch. 6]. The existence criteria in Theorem 2.1 is the most pertinent when we employ inverse regression for ridge recovery in Section 4.

There are two useful properties of the central subspace that enable convenient transformations. The first involves the effect of affine transformations in the predictor space. Let $\mathbf{z} = \mathbf{B}\mathbf{x} + \mathbf{b}$ for full rank $\mathbf{B} \in \mathbb{R}^{m \times m}$ and $\mathbf{x} \in \mathbb{R}^m$. If $\text{colspan}(\mathbf{A}) = \mathcal{S}_{y|\mathbf{x}}$ for some $\mathbf{A} \in \mathbb{R}^{m \times n}$, then $\text{colspan}(\mathbf{B}^{-\top} \mathbf{A}) = \mathcal{S}_{y|\mathbf{z}}$ [13]. This allows us to make the following assumption about the predictor space without loss of generality.

ASSUMPTION 1 (Standardized predictors). *Assume that \mathbf{x} is standardized such that*

$$(2.4) \quad \mathbb{E}[\mathbf{x}] = \mathbf{0}, \quad \mathbb{C} \text{ov}[\mathbf{x}] = \mathbf{I}.$$

The second property involves mappings of the response. Let $h : \mathbb{R} \rightarrow \mathbb{R}$ be a function applied to the responses that produces a new regression problem, $\{[\mathbf{x}_i^\top, h(y_i)]\}$, $i = 1, \dots, N$. The central subspace associated with the new regression problem is contained within the original central subspace,

$$(2.5) \quad \mathcal{S}_{h(y)|\mathbf{x}} \subseteq \mathcal{S}_{y|\mathbf{x}},$$

with equality holding when h is strictly monotone [15]. Equation (2.5) is essential for studying the *slicing*-based algorithms, SIR and SAVE, for estimating the central subspace, where the mapping h partitions the response space; see Sections 2.1 and 2.2.

The goal of SDR is to estimate the central subspace for the regression from the given response/predictor pairs.

PROBLEM 1 (SDR problem). *Given response/predictor pairs $\{[\mathbf{x}_i^\top, y_i]\}$, with $i = 1, \dots, N$, assumed to be independent draws from a random vector $[\mathbf{x}^\top, y]$ with joint density $p_{\mathbf{x},y}$, compute a basis $\mathbf{A} \in \mathbb{R}^{m \times n}$ for the central subspace $\mathcal{S}_{y|\mathbf{x}}$ of the random variable $y|\mathbf{x}$.*

Next we review two algorithms for Problem 1—sliced inverse regression [37] and sliced average variance estimation [17]. These algorithms use the given regression data to approximate population moment matrices of the *inverse regression* $\mathbf{x}|y$.

2.1. Sliced inverse regression. Sliced inverse regression (SIR) [37] is an algorithm for approximating the matrix

$$(2.6) \quad \mathbf{C}_{\text{IR}} = \mathbb{C} \text{ov}[\mathbb{E}[\mathbf{x}|y]]$$

using the given predictor/response pairs. \mathbf{C}_{IR} is defined by the *inverse regression function* $\mathbb{E}[\mathbf{x}|y]$, which draws a curve through the m -dimensional predictor space parameterized by the scalar-valued response. If the given regression problem satisfies the *linearity condition* [37], then

$$(2.7) \quad \text{colspan}(\mathbf{C}_{\text{IR}}) \subseteq \mathcal{S}_{y|\mathbf{x}}.$$

In words, the column space of \mathbf{C}_{IR} is a subset of the central subspace for the regression. The linearity condition is satisfied when the marginal density $p_{\mathbf{x}}$ is elliptically symmetric (e.g., a multivariate standard Gaussian) [21].

SIR approximates \mathbf{C}_{IR} using given predictor/response pairs by partitioning (i.e., *slicing*) the response space. Consider a partition of the observed response space,

$$(2.8) \quad \min_{1 \leq i \leq N} y_i = \tilde{y}_0 < \tilde{y}_1 < \dots < \tilde{y}_{R-1} < \tilde{y}_R = \max_{1 \leq i \leq N} y_i,$$

and let $J_r = [\tilde{y}_{r-1}, \tilde{y}_r]$ denote the r th partition for $r = 1, \dots, R$. Define the function

$$(2.9) \quad h(y) = r \quad \text{for } y \in J_r.$$

Applying h to the given responses creates a new regression problem $\{[\mathbf{x}_i^\top, h(y_i)]\}$, where (2.6) becomes

$$(2.10) \quad \mathbf{C}_{\text{SIR}} = \mathbb{C} \text{ov}[\mathbb{E}[\mathbf{x}|h(y)]] .$$

The notation \mathbf{C}_{SIR} emphasizes that this matrix is with respect to the sliced version of the original regression problem. Combining (2.7) and (2.5),

$$(2.11) \quad \text{colspan}(\mathbf{C}_{\text{SIR}}) \subseteq \mathcal{S}_{h(y)|\mathbf{x}} \subseteq \mathcal{S}_{y|\mathbf{x}}.$$

The sliced partition of the response space and the sliced mapping h bin the predictor/response pairs to enable sample estimates of $\mathbb{E}[\mathbf{x}|r]$ for $r = 1, \dots, R$. This is the basic idea behind the SIR algorithm; see Algorithm 2.1. Note that if the response is discrete, then Algorithm 2.1 produces the maximum likelihood estimator of the central subspace [16].

Algorithm 2.1 Sliced inverse regression [37]

Given: N samples $\{[\mathbf{x}_i^\top, y_i]\}$, $i = 1, \dots, N$, drawn independently according to $p_{\mathbf{x},y}$.

1. Partition the response space as in (2.8), and let $J_r = [\tilde{y}_{r-1}, \tilde{y}_r]$ for $r = 1, \dots, R$. Let $\mathcal{I}_r \subset \{1, \dots, N\}$ be the set of indices i for which $y_i \in J_r$ and define N_r to be the cardinality of \mathcal{I}_r .
2. For $r = 1, \dots, R$, compute the sample mean $\hat{\boldsymbol{\mu}}_h(r)$ of the predictors whose associated responses are in J_r ,

$$(2.12) \quad \hat{\boldsymbol{\mu}}_h(r) = \frac{1}{N_r} \sum_{i \in \mathcal{I}_r} \mathbf{x}_i.$$

3. Compute the weighted sample covariance matrix

$$(2.13) \quad \hat{\mathbf{C}}_{\text{SIR}} = \frac{1}{N} \sum_{r=1}^R N_r \hat{\boldsymbol{\mu}}_h(r) \hat{\boldsymbol{\mu}}_h(r)^\top.$$

4. Compute the eigendecomposition,

$$(2.14) \quad \hat{\mathbf{C}}_{\text{SIR}} = \hat{\mathbf{W}} \hat{\boldsymbol{\Lambda}} \hat{\mathbf{W}}^\top,$$

where the eigenvalues are in descending order $\hat{\lambda}_1 \geq \hat{\lambda}_2 \geq \dots \geq \hat{\lambda}_m \geq 0$ and the eigenvectors are orthonormal.

5. Let $\hat{\mathbf{A}} \in \mathbb{R}^{m \times n}$ be the first n eigenvectors of $\hat{\mathbf{C}}_{\text{SIR}}$; return $\hat{\mathbf{A}}$.
-

Eigenvectors of \mathbf{C}_{SIR} associated with nonzero eigenvalues provide a basis for the SIR subspace, $\text{colspan}(\mathbf{C}_{\text{SIR}})$. If the approximated eigenvalues $\hat{\lambda}_{n+1}, \dots, \hat{\lambda}_m$ from Algorithm 2.1 are small, then $m \times n$ matrix $\hat{\mathbf{A}}$ approximates a basis for this subspace. However, determining the appropriate value of n requires care. Li [37] and Cook [17] propose significance tests based on the distribution of the average of the $m-n$ trailing estimated eigenvalues. These testing methods also apply to the SAVE algorithm in Section 2.2.

For a fixed number of slices, SIR has been shown to be $N^{-1/2}$ -consistent for approximating $\text{colspan}(\mathbf{C}_{\text{SIR}})$ [37]. In principle, increasing the number of slices may provide improved estimation of the central DRS. However, in practice, SIR's success is relatively insensitive to the number of slices. The number of slices should be chosen such that there are enough samples in each slice to estimate the conditional expectations accurately. For this reason, Li [37] suggests constructing slices such that the response samples are distributed nearly equally.

2.2. Sliced average variance estimation. SAVE uses the variance of the inverse regression. Li [37] recognized the potential for $\mathbb{C} \text{ov} [\mathbf{x}|y]$ to provide insights into the central subspace by noting that, under Assumption 1,

$$(2.15) \quad \mathbb{E} [\mathbb{C} \text{ov} [\mathbf{x}|y]] = \mathbb{C} \text{ov} [\mathbf{x}] - \mathbb{C} \text{ov} [\mathbb{E} [\mathbf{x}|y]] = \mathbf{I} - \mathbb{C} \text{ov} [\mathbb{E} [\mathbf{x}|y]].$$

Equation (2.15) implies that $\mathbb{E} [\mathbf{I} - \mathbb{C} \text{ov} [\mathbf{x}|y]]$ may be useful in addressing Problem 1. Cook suggests using $\mathbb{E} [(\mathbf{I} - \mathbb{C} \text{ov} [\mathbf{x}|y])^2]$, which has nonnegative eigenvalues [17]. Define

$$(2.16) \quad \mathbf{C}_{\text{AVE}} = \mathbb{E} [(\mathbf{I} - \mathbb{C} \text{ov} [\mathbf{x}|y])^2].$$

Under the *linearity condition* [37] and the *constant covariance condition* [15], the column space of \mathbf{C}_{AVE} is contained within the central subspace,

$$(2.17) \quad \text{colspan}(\mathbf{C}_{\text{AVE}}) \subseteq \mathcal{S}_{y|\mathbf{x}}.$$

Both of these conditions are satisfied when the predictors have an elliptically symmetric marginal density [21].

Using the partition (2.8) and the map (2.9),

$$(2.18) \quad \mathbf{C}_{\text{SAVE}} = \mathbb{E} [(\mathbf{I} - \mathbb{C} \text{ov} [\mathbf{x}|h(y)])^2].$$

The notation \mathbf{C}_{SAVE} indicates application to the sliced version of the original regression problem. Combining (2.17) and (2.5),

$$(2.19) \quad \text{colspan}(\mathbf{C}_{\text{SAVE}}) \subseteq \mathcal{S}_{h(y)|\mathbf{x}} \subseteq \mathcal{S}_{y|\mathbf{x}}.$$

Algorithm 2.2 shows the SAVE algorithm, which computes a basis for the column span of the sample estimate $\hat{\mathbf{C}}_{\text{SAVE}}$. This basis is a $N^{-1/2}$ -consistent estimate of $\text{colspan}(\mathbf{C}_{\text{SAVE}})$ [15]. Increasing the number of slices improves the estimate but suffers the same drawbacks as SIR. In practice, SAVE performs poorly compared to SIR when few predictor/response pairs are available. This is due to difficulties approximating the covariances within the slices using too few samples. For this reason, Cook [16] suggests trying both methods to approximate the central DRS.

3. Ridge functions. The input/output map of a computer simulation is best modeled by a deterministic function,

$$(3.1) \quad y = f(\mathbf{x}), \quad \mathbf{x} \in \mathbb{R}^m, \quad y \in \mathbb{R}.$$

We assume the domain of f is equipped with a known input probability measure $\pi_{\mathbf{x}}$. In an uncertainty quantification context, $\pi_{\mathbf{x}}$ encodes uncertainty in the physical inputs. We assume $\pi_{\mathbf{x}}$ admits a density function $p_{\mathbf{x}} : \mathbb{R}^m \rightarrow \mathbb{R}^+$ and that the m inputs are independent. Common choices for $p_{\mathbf{x}}$ include a multivariate Gaussian and a uniform density over a hyperrectangle. The pair f and $\pi_{\mathbf{x}}$ induces an unknown push-forward probability measure on the output space, which we denote by π_y .

Translating sufficient dimension reduction to deterministic functions naturally leads to *ridge functions* [44].

DEFINITION 3 (Ridge function [44]). *A function $f : \mathbb{R}^m \rightarrow \mathbb{R}$ is a ridge function if there exists a matrix $\mathbf{A} \in \mathbb{R}^{m \times n}$ with $n < m$ and a function $g : \mathbb{R}^n \rightarrow \mathbb{R}$ such that*

$$(3.2) \quad y = f(\mathbf{x}) = g(\mathbf{A}^\top \mathbf{x}).$$

The columns of \mathbf{A} are the directions of the ridge function and $g : \mathbb{R}^n \rightarrow \mathbb{R}$ is the ridge profile.

Algorithm 2.2 Sliced average variance estimation [15]

Given: N samples $\{[\mathbf{x}_i^\top, y_i]\}, i = 1, \dots, N$, drawn independently according to $p_{\mathbf{x}, y}$.

1. Define a partition of the response space as in (2.8), and let $J_r = [\tilde{y}_{r-1}, \tilde{y}_r]$ for $r = 1, \dots, R$. Let $\mathcal{I}_r \subset \{1, \dots, N\}$ be the set of indices i for which $y_i \in J_r$ and define N_r to be the cardinality of \mathcal{I}_r .
2. For $r = 1, \dots, R$,
 - (a) Compute the sample mean $\hat{\boldsymbol{\mu}}_h(r)$ of the predictors whose associated responses are in the J_r ,

$$(2.20) \quad \hat{\boldsymbol{\mu}}_h(r) = \frac{1}{N_r} \sum_{i \in \mathcal{I}_r} \mathbf{x}_i.$$

- (b) Compute the sample covariance $\hat{\boldsymbol{\Sigma}}_h(r)$ of the predictors whose associated responses are in J_r ,

$$(2.21) \quad \hat{\boldsymbol{\Sigma}}_h(r) = \frac{1}{N_r - 1} \sum_{i \in \mathcal{I}_r} (\mathbf{x}_i - \hat{\boldsymbol{\mu}}_h(r)) (\mathbf{x}_i - \hat{\boldsymbol{\mu}}_h(r))^\top$$

3. Compute the matrix,

$$(2.22) \quad \hat{\mathbf{C}}_{\text{SAVE}} = \frac{1}{N} \sum_{r=1}^R N_r \left(\mathbf{I} - \hat{\boldsymbol{\Sigma}}_h(r) \right)^2.$$

4. Compute the eigendecomposition,

$$(2.23) \quad \hat{\mathbf{C}}_{\text{SAVE}} = \hat{\mathbf{W}} \hat{\boldsymbol{\Lambda}} \hat{\mathbf{W}}^\top,$$

where the eigenvalues are in descending order $\hat{\lambda}_1 \geq \hat{\lambda}_2 \geq \dots \geq \hat{\lambda}_m \geq 0$ and the eigenvectors are orthonormal.

5. Let $\hat{\mathbf{A}} \in \mathbb{R}^{m \times n}$ be the first n eigenvectors of $\hat{\mathbf{C}}_{\text{SAVE}}$; return $\hat{\mathbf{A}}$.
-

A ridge function is nominally a function of m inputs, but it is intrinsically a function of $n < m$ derived inputs. The term *ridge function* sometimes refers to the $n = 1$ case, and $n > 1$ is called a *generalized ridge functions* [44]. We do not distinguish between the $n = 1$ and $n > 1$ cases and refer to all such functions as ridge functions for convenience.

Ridge functions appear in a wide range of computational techniques. For example, projection pursuit regression uses a regression model that is a sum of n one-dimensional ridge functions, $\sum_{i=1}^n g_i(\mathbf{a}_i^\top \mathbf{x})$, where each g_i is a spline or other non-parametric model [24]. Neural network nodes use functions of the form $\sigma(\mathbf{W}^\top \mathbf{x} + \mathbf{b})$, where \mathbf{W} is a matrix of weights from the previous layer of neurons, \mathbf{b} is a bias term for the model, and $\sigma(\cdot)$ is an activation function [30].

Ridge functions are good low-dimensional models for functions that exhibit off-axis anisotropic dependence on the inputs since they are constant along the $m - n$ directions of the input space that are orthogonal to the columns of \mathbf{A} . Consider a vector $\mathbf{w} \in \text{null}(\mathbf{A}^\top)$. Then, for any $\mathbf{x} \in \mathbb{R}^m$,

$$(3.3) \quad f(\mathbf{x} + \mathbf{w}) = g(\mathbf{A}^\top(\mathbf{x} + \mathbf{w})) = g(\mathbf{A}^\top \mathbf{x} + \mathbf{0}) = g(\mathbf{A}^\top \mathbf{x}) = f(\mathbf{x}).$$

We refer to the problem of finding the directions of a ridge function as *ridge recovery*.

PROBLEM 2 (Ridge recovery). *Given a query-able deterministic function $f : \mathbb{R}^m \rightarrow \mathbb{R}$ and an input probability measure $\pi_{\mathbf{x}}$, find $\mathbf{A} \in \mathbb{R}^{m \times n}$ with $n < m$ such that*

$$(3.4) \quad f(\mathbf{x}) = g(\mathbf{A}^\top \mathbf{x}).$$

Recent papers in signal processing and approximation theory propose and analyze algorithms for ridge recovery. Cohen et al. [6] consider the case of $n = 1$ with conditions on the ridge direction. Fornasier, Schnass, and Vybiral [23] propose an algorithm for general $n < m$ under conditions on \mathbf{A} . Tyahi and Cevher [54] extend the approximation results from Fornasier et al. to more general \mathbf{A} 's.

Note that the ridge recovery problem is distinct from ridge approximation [9, 32], where the goal is to find \mathbf{A} and construct g that minimize the approximation error for a given f .¹ Inverse regression may be useful for ridge approximation or identifying near-ridge structure in a given function, but pursuing these ideas is beyond the scope of this manuscript. Li, Lin, and Li [40] distinguish between an “ideal scenario”—which loosely corresponds to ridge recovery and where they can prove certain convergence results for inverse regression—and the “general setting”—where they apply inverse regression as a heuristic in numerical examples.

4. Inverse regression as ridge recovery. This section develops SIR (Algorithm 2.1) and SAVE (Algorithm 2.2) as tools for ridge recovery (Problem 2). The next theorem connects the dimension reduction subspace (Definition 1) to the ridge directions (Definition 3).

THEOREM 4.1. *Let (Ω, Σ, P) be a probability triple. Suppose that $\mathbf{x} : \Omega \rightarrow \mathbb{R}^m$ and $y : \Omega \rightarrow \mathbb{R}$ are random variables related by a measurable function $f : \mathbb{R}^m \rightarrow \mathbb{R}$ so that $y = f(\mathbf{x})$. Let $\mathbf{A} \in \mathbb{R}^{m \times n}$ be a constant matrix. Then $y \perp\!\!\!\perp \mathbf{x} | \mathbf{A}^\top \mathbf{x}$ if and only if $y = g(\mathbf{A}^\top \mathbf{x})$ where $g : \mathbb{R}^n \rightarrow \mathbb{R}$ is a measurable function.*

The proof is in Appendix A.1. Theorem 4.1 states that conditional independence of the inputs and output in a deterministic function is equivalent to the function being a ridge function. This provides a subspace-based perspective on ridge functions that uses the DRS as the foundation. That is, the directions of the ridge function are relatively unimportant compared to the subspace they span when capturing ridge structure of f with sufficient dimension reduction.

The central subspace (Definition 2) corresponds to the unique subspace of smallest dimension that completely describes the ridge structure of f . Moreover, our focused concern on the subspace instead of the precise basis implies that we can assume standardized inputs \mathbf{x} (as in Assumption 1) without loss of generality, which simplifies discussion of the inverse conditional moment matrices that define the SIR and SAVE subspaces for ridge recovery.

Theorem 2.1 guarantees existence of the central subspace in regression when the marginal density of the predictors has convex support. However, this condition is typically difficult or impossible to verify for the regression problem. In contrast, the deterministic function is accompanied by a known input measure $\pi_{\mathbf{x}}$ with density function $p_{\mathbf{x}}$. In practice, a relatively non-informative measure is used such as a multivariate Gaussian or uniform density on a hyper-rectangle defined by the ranges of

¹Regarding nomenclature, neither ridge recovery nor ridge approximation is related to ridge regression, where Tikhonov regularization is applied to the regression model coefficients [31, Chapter 3.4].

each physical input parameter. Such choices for modeling input uncertainty satisfy Theorem 2.1 and guarantee the existence of the central subspace.

The input probability measure can influence the structure of the central subspace. For example, let $\mathbf{a}, \mathbf{b} \in \mathbb{R}^m$ be constant vectors pointing in different directions and consider the function

$$(4.1) \quad y = f(\mathbf{x}) = \begin{cases} (\mathbf{a}^\top \mathbf{x})^2 & \text{if } \mathbf{x}_i > 0 \text{ for } i = 1, \dots, m \\ (\mathbf{b}^\top \mathbf{x})^2 & \text{otherwise.} \end{cases}$$

If $\pi_{\mathbf{x}}$ has a density function with support only for positive values of \mathbf{x} (e.g., uniform over $[0, 1]^m$), then the central subspace is $\text{span}\{\mathbf{a}\}$. Alternatively, if the input density has support over all of \mathbb{R}^m (e.g., multivariate Gaussian), then the central subspace is $\text{span}\{\mathbf{a}, \mathbf{b}\}$. For this reason, we write the central subspace for a deterministic function as $\mathcal{S}_{f, \pi_{\mathbf{x}}}$ to emphasize that this subspace is a property of the given function and input probability measure.

For deterministic functions, the translation of the inverse regression $\mathbf{x}|y$ (see Section 2) is the inverse image of f for the output value y ,

$$(4.2) \quad f^{-1}(y) = \{\mathbf{x} \in \mathbb{R}^m : f(\mathbf{x}) = y\}.$$

Unlike the random vector inverse regression, f^{-1} is a fixed set determined by f 's contours. Furthermore, the inverse image begets the conditional probability measure $\pi_{\mathbf{x}|y}$, which is the restriction of $\pi_{\mathbf{x}}$ to the set $f^{-1}(y)$ [5].

4.1. Sliced inverse regression for ridge recovery. For deterministic functions, we can write \mathbf{C}_{IR} from (2.6) as an integral:

$$(4.3) \quad \mathbf{C}_{\text{IR}} = \int \boldsymbol{\mu}(y) \boldsymbol{\mu}(y)^\top d\pi_y(y)$$

where the conditional expectation over the inverse image $f^{-1}(y)$ is

$$(4.4) \quad \boldsymbol{\mu}(y) = \int \mathbf{x} d\pi_{\mathbf{x}|y}(\mathbf{x}).$$

This term represents the average of all input values that map to a fixed value of the output.

To understand how \mathbf{C}_{IR} can be used for dimension reduction in deterministic functions, consider the following. For $\mathbf{w} \in \mathbb{R}^m$ with unit norm,

$$(4.5) \quad \mathbf{w}^\top \mathbf{C}_{\text{IR}} \mathbf{w} = \mathbf{w}^\top \left(\int \boldsymbol{\mu}(y) \boldsymbol{\mu}(y)^\top d\pi_y(y) \right) \mathbf{w} = \int (\boldsymbol{\mu}(y)^\top \mathbf{w})^2 d\pi_y(y).$$

If $\mathbf{w} \in \text{null}(\mathbf{C}_{\text{IR}})$, then one possibility is that $\boldsymbol{\mu}(y)$ is orthogonal to \mathbf{w} for all y . The following theorem relates this case to possible ridge structure in f .

THEOREM 4.2. *Let $f : \mathbb{R}^m \rightarrow \mathbb{R}$ with input probability measure $\pi_{\mathbf{x}}$ admit a central subspace $\mathcal{S}_{f, \pi_{\mathbf{x}}}$, and assume $\pi_{\mathbf{x}}$ admits an elliptically symmetric and standardized density function. Then, $\text{colspan}(\mathbf{C}_{\text{IR}}) \subseteq \mathcal{S}_{f, \pi_{\mathbf{x}}}$.*

See Appendix A.2 for the proof. Theorem 4.2 shows that a basis for the range of \mathbf{C}_{IR} can be used to estimate f 's central subspace. However, this idea has two important limitations. First, by (4.5), we can write the inner product in the rightmost integrand in terms of the cosine of the angle between the vectors $\boldsymbol{\mu}(y)$ and \mathbf{w} ,

$$(4.6) \quad \mathbf{w}^\top \mathbf{C}_{\text{IR}} \mathbf{w} = \int \|\boldsymbol{\mu}(y)\|_2^2 \cos^2(\theta(y)) d\pi_y(y),$$

where $\theta(y)$ is the angle between $\boldsymbol{\mu}(y)$ and \mathbf{w} . Theorem 4.2 uses orthogonality of $\boldsymbol{\mu}(y)$ and \mathbf{w} (i.e., $\cos(\theta(y)) = 0$ for all y) to show containment of the column space of \mathbf{C}_{IR} within the central subspace; however, the integrand in (4.6) also contains the squared 2-norm of $\boldsymbol{\mu}(y)$, which does not depend on \mathbf{w} . If $\boldsymbol{\mu}(y) = \mathbf{0}$ for all y , then $\mathbf{w}^\top \mathbf{C}_{\text{IR}} \mathbf{w} = 0$ for all \mathbf{w} . Consider the following example.

EXAMPLE 1. Assume $\mathbf{x} \in \mathbb{R}^2$ is weighted with a bivariate standard Gaussian. Let $y = f(\mathbf{x}) = x_1 x_2$. For any value of y , $\mathbf{x} \in f^{-1}(y)$ implies $-\mathbf{x} \in f^{-1}(y)$. Therefore, $\boldsymbol{\mu}(y) = \mathbf{0}$ for all y , and $\mathbf{C}_{\text{IR}} = \mathbf{0}$. But y is not constant over \mathbb{R}^2 . Thus, $\{\mathbf{0}\} = \text{colspan}(\mathbf{C}_{\text{IR}}) \subset \mathcal{S}_{f, \pi_{\mathbf{x}}} = \mathbb{R}^2$.

This example shows how \mathbf{C}_{IR} , as a tool for ridge recovery, can mislead the practitioner by suggesting ridge structure in a function that is not a ridge function. This could lead one to ignore input space directions that should not be ignored. Note that if we shift the function such that $y = f(\mathbf{x}) = (x_1 + c_1)(x_2 + c_2)$ for some constants $c_1, c_2 \neq 0$, then the symmetry is broken and $\boldsymbol{\mu}(y) \neq \mathbf{0}$ for all y . In this case, \mathbf{C}_{IR} will recover the central subspace (i.e., all of \mathbb{R}^2).

The second limitation of \mathbf{C}_{IR} for ridge recovery follows from the required elliptic symmetry of the input density $p_{\mathbf{x}}$. This assumption is satisfied if $p_{\mathbf{x}}$ is a multivariate Gaussian, but it is violated when the density is uniform over the m -dimension hypercube. If f is a ridge function and $\mathbf{w} \in \text{null}(\mathbf{A}^\top)$, then $\mathbf{x} \in f^{-1}(y)$ implies $\mathbf{x} + \mathbf{w} \in f^{-1}(y)$ so that $f^{-1}(y)$ can be expressed as the union of lines parallel to \mathbf{w} . If the inputs are weighted by an elliptically symmetric density, then the expectation over $f^{-1}(y)$ will be centered such that $\boldsymbol{\mu}(y)$ is orthogonal to \mathbf{w} . If the inputs do not have an elliptically symmetric density, then the weighting can cause the conditional expectation to deviate in the direction of \mathbf{w} . The magnitude of this deviation also depends on the magnitude of the conditional expectation $\|\boldsymbol{\mu}(y)\|_2$.

Next, we examine the sliced approximation of \mathbf{C}_{IR} . Recall the output partition from (2.8) and the slicing map $h(y)$ (2.9). Applying h to the deterministic function $y = f(\mathbf{x})$ produces the discretized function $r = h(y) = h(f(\mathbf{x}))$, where $r \in \{1, \dots, R\}$. The output space of h is weighted by the probability mass function

$$(4.7) \quad \omega(r) = \int_{J_r} d\pi_y(y), \quad r \in \{1, \dots, R\}.$$

Without loss of generality, we assume that the slices are constructed such that $\omega(r) > 0$ for all r . If $\omega(r) = 0$ for some r , then we can combine this slice with an adjacent slice. The conditional expectation for the sliced output is

$$(4.8) \quad \boldsymbol{\mu}_h(r) = \int \mathbf{x} d\pi_{\mathbf{x}|r}(\mathbf{x}),$$

where $\pi_{\mathbf{x}|r}$ is the conditional measure defined over the set $f^{-1}(h^{-1}(r)) = \{\mathbf{x} \in \mathbb{R}^m : h(f(\mathbf{x})) = h(y) = r\}$. Using (4.7) and (4.8), the sliced version of \mathbf{C}_{IR} is

$$(4.9) \quad \mathbf{C}_{\text{SIR}} = \sum_{r=1}^R \omega(r) \boldsymbol{\mu}_h(r) \boldsymbol{\mu}_h(r)^\top.$$

By Theorem 4.1, properties of the central subspace extend to the ridge recovery problem. This includes containment of the central subspace under any mapping of the output,

$$(4.10) \quad \text{colspan}(\mathbf{C}_{\text{SIR}}) \subseteq \mathcal{S}_{h \circ f, \pi_{\mathbf{x}}} \subseteq \mathcal{S}_{f, \pi_{\mathbf{x}}}.$$

By approximating \mathbf{C}_{SIR} , we obtain an approximation of part of f 's central subspace. An important corollary of (4.10) is that the rank of \mathbf{C}_{SIR} is bounded above by the dimension of $\mathcal{S}_{f, \pi_{\mathbf{x}}}$.

Note that \mathbf{C}_{SIR} from (4.9) is a finite sum approximation of the integral in \mathbf{C}_{IR} from (4.3). Since $f^{-1}(h^{-1}(r)) = \cup_{y \in J_r} f^{-1}(y)$, then $\boldsymbol{\mu}_h(r)$ is the average of the conditional expectations with $y \in J_r$. That is,

$$(4.11) \quad \boldsymbol{\mu}_h(r) = \int_{J_r} \boldsymbol{\mu}(y) d\pi_y(y).$$

Therefore, \mathbf{C}_{SIR} approximates \mathbf{C}_{IR} by a weighted sum of the average values of $\boldsymbol{\mu}(y)$ within each slice. If $\boldsymbol{\mu}(y)$ is continuous almost everywhere with respect to π_y , then \mathbf{C}_{IR} is Riemann-integrable [22, Ch. 2]. This ensures that sum approximations using the supremum and infimums of $\boldsymbol{\mu}(y)$ over each slice converge to the same value. By the sandwich theorem, the average value will converge to this value as well [1]. Therefore, \mathbf{C}_{SIR} is a Riemann sum approximation of \mathbf{C}_{IR} ; as the number of slices R increases, \mathbf{C}_{SIR} converges to \mathbf{C}_{IR} .

We turn attention to asymptotic convergence of Algorithm 2.1 for ridge recovery. To generate the data for Algorithm 2.1, we choose N points $\{\mathbf{x}_i\}$ in the input space consistent with $\pi_{\mathbf{x}}$. For each \mathbf{x}_i , we query the function to produce the corresponding output $y_i = f(\mathbf{x}_i)$. In the computational science context, this corresponds to running the simulation model at particular sets of inputs. If we choose each \mathbf{x}_i independently according to $\pi_{\mathbf{x}}$, then we can analyze SIR as a Monte Carlo method for estimating \mathbf{C}_{SIR} from (4.9). Given the input/output pairs, Algorithm 2.1 constructs the random matrix $\hat{\mathbf{C}}_{\text{SIR}}$. To be clear, $\hat{\mathbf{C}}_{\text{SIR}}$ is a random estimate of \mathbf{C}_{SIR} because of how we chose the points $\{\mathbf{x}_i\}$ —not because of any randomness in the map f . Eigenpairs derived from $\hat{\mathbf{C}}_{\text{SIR}}$ are also random, and the convergence analysis for Algorithm 2.1 is probabilistic.

The convergence depends on the smallest number of samples per slice over all the slices:

$$(4.12) \quad N_{r_{\min}} = \min_{1 \leq r \leq R} N_r,$$

where N_r is from Algorithm 2.1. Recall that the slices are assumed to be constructed such that $\omega(r) > 0$. Thus, $N_{r_{\min}} > 0$ with probability 1 as $N \rightarrow \infty$. The following theorem shows that the eigenvalues of $\hat{\mathbf{C}}_{\text{SIR}}$ converge to those of \mathbf{C}_{SIR} in a mean-squared sense.

THEOREM 4.3. *Assume that Algorithm 2.1 has been applied to the data set $\{[\mathbf{x}_i^\top, y_i]\}$, with $i = 1, \dots, N$, where the \mathbf{x}_i are drawn independently according to $\pi_{\mathbf{x}}$ and $y_i = f(\mathbf{x}_i)$ are point evaluations of f . Then, for $k = 1, \dots, m$,*

$$(4.13) \quad \mathbb{E} \left[\left(\lambda_k(\mathbf{C}_{\text{SIR}}) - \lambda_k(\hat{\mathbf{C}}_{\text{SIR}}) \right)^2 \right] = \mathcal{O}(N_{r_{\min}}^{-1})$$

where $\lambda_k(\cdot)$ denotes the k th eigenvalue of the given matrix.

See Appendix A.3 for the proof. In words, the mean-squared error in the eigenvalues of $\hat{\mathbf{C}}_{\text{SIR}}$ decays at a $N_{r_{\min}}^{-1}$ rate. Since $\omega(r) > 0$ for all r , $N_{r_{\min}} \rightarrow \infty$ as $N \rightarrow \infty$. Moreover, the convergence rate suggests that one should choose the slices in Algorithm 2.1 such that the same number of samples appears in each slice. This maximizes $N_{r_{\min}}$ and reduces the error in the eigenvalues.

An important consequence of Theorem 4.3 is that the column space of the finite-sample $\hat{\mathbf{C}}_{\text{SIR}}$ is not contained in f 's central subspace. In fact, due to finite sampling, $\hat{\mathbf{C}}_{\text{SIR}}$ is not precisely low-rank. With a fixed number of samples, it is difficult to distinguish the effects of finite sampling from actual variability in f . However, the eigenvalue convergence implies that one can potentially devise practical tests for low-rank-ness based on sets of samples with increasing size.

The next theorem shows the value of understanding the approximation errors in the eigenvalues for quantifying the approximation errors in the subspaces. We measure convergence of the subspace estimates using the subspace distance [29, Chapter 2.5],

$$(4.14) \quad \text{dist} \left(\text{colspan}(\mathbf{A}), \text{colspan}(\hat{\mathbf{A}}) \right) = \left\| \mathbf{A}\mathbf{A}^\top - \hat{\mathbf{A}}\hat{\mathbf{A}}^\top \right\|_2,$$

where $\mathbf{A}, \hat{\mathbf{A}}$ are the first n eigenvectors of \mathbf{C}_{SIR} and $\hat{\mathbf{C}}_{\text{SIR}}$, respectively. The distance metric (4.14) is the principal angle between the subspaces $\text{colspan}(\mathbf{A})$ and $\text{colspan}(\hat{\mathbf{A}})$.

THEOREM 4.4. *Assume the same conditions from Theorem 4.3. Then, for sufficiently large N ,*

$$(4.15) \quad \text{dist} \left(\text{colspan}(\mathbf{A}), \text{colspan}(\hat{\mathbf{A}}) \right) = \frac{1}{\lambda_n(\mathbf{C}_{\text{SIR}}) - \lambda_{n+1}(\mathbf{C}_{\text{SIR}})} \mathcal{O}_p(N_{r_{\min}}^{-1/2}).$$

Appendix A.4 contains the proof. The subspace error decays with asymptotic rate $N_{r_{\min}}^{-1/2}$. The more interesting result from Theorem 4.4 is the inverse relationship between the subspace error and the magnitude of the gap between the n th and $(n+1)$ th eigenvalues. That is, a large gap between eigenvalues suggests a better estimate of the subspace for a fixed number of samples. We do not hide this factor in the \mathcal{O} notation to emphasize the importance of Theorem 4.3, which provides insights into the accuracy of the estimated eigenvalues of \mathbf{C}_{SIR} .

4.2. SAVE for ridge recovery. Similar to (4.3), we express \mathbf{C}_{AVE} from (2.16) as an integral,

$$(4.16) \quad \mathbf{C}_{\text{AVE}} = \int (\mathbf{I} - \boldsymbol{\Sigma}(y))^2 d\pi_y(y).$$

The conditional covariance $\boldsymbol{\Sigma}(y)$ in (4.16) is an integral against the conditional probability measure $\pi_{\mathbf{x}|y}$,

$$(4.17) \quad \boldsymbol{\Sigma}(y) = \int (\mathbf{x} - \boldsymbol{\mu}(y)) (\mathbf{x} - \boldsymbol{\mu}(y))^\top d\pi_{\mathbf{x}|y}(\mathbf{x}).$$

To see the relationship between the \mathbf{C}_{AVE} matrix and ridge functions, let $\mathbf{w} \in \mathbb{R}^m$ with unit norm:

$$(4.18) \quad \mathbf{w}^\top \mathbf{C}_{\text{AVE}} \mathbf{w} = \mathbf{w}^\top \left(\int (\mathbf{I} - \boldsymbol{\Sigma}(y))^2 d\pi_y(y) \right) \mathbf{w} = \int \|(\mathbf{I} - \boldsymbol{\Sigma}(y)) \mathbf{w}\|_2^2 d\pi_y(y).$$

Equation (4.18) relates the column space of \mathbf{C}_{AVE} to the ridge structure in f .

THEOREM 4.5. *Let $f : \mathbb{R}^m \rightarrow \mathbb{R}$ with input probability measure $\pi_{\mathbf{x}}$ admit a central subspace $\mathcal{S}_{f, \pi_{\mathbf{x}}}$, and assume $\pi_{\mathbf{x}}$ admits an elliptically symmetric and standardized density function. Then, $\text{colspan}(\mathbf{C}_{\text{AVE}}) \subseteq \mathcal{S}_{f, \pi_{\mathbf{x}}}$.*

See the proof in Appendix A.5. This result shows the usefulness of \mathbf{C}_{AVE} for revealing ridge structure in deterministic functions: by estimating the column space of \mathbf{C}_{AVE} , we obtain an estimate of a subspace of f 's central subspace. However, \mathbf{C}_{AVE} suffers two similar pitfalls as \mathbf{C}_{IR} . First, \mathbf{C}_{AVE} can mislead the practitioner by suggesting ridge structure that does not exist (i.e., when $\text{colspan}(\mathbf{C}_{\text{AVE}}) \subset \mathcal{S}_{f, \pi_{\mathbf{x}}}$), as the following example illustrates.

EXAMPLE 2. Assume $\mathbf{x} \in \mathbb{R}^2$ is weighted by a bivariate standard Gaussian. Let $y = f(\mathbf{x}) = \frac{1}{\sqrt{2}}x_1^2 + x_2$. Then,

$$(4.19) \quad \int \mathbf{x}\mathbf{x}^\top d\pi_{\mathbf{x}|y}(\mathbf{x}) = \begin{bmatrix} \alpha(y) & 0 \\ 0 & y^2 - \sqrt{2}y + \frac{3}{2} \end{bmatrix},$$

where $\alpha(y) = \sqrt{2} \int |y - x_2| d\pi_{x_2|y}(x_2)$, and

$$(4.20) \quad \boldsymbol{\mu}(y) = \int \mathbf{x} d\pi_{\mathbf{x}|y}(\mathbf{x}) = \begin{bmatrix} 0 \\ y - \frac{1}{\sqrt{2}} \end{bmatrix}.$$

Then

$$(4.21) \quad \begin{aligned} \boldsymbol{\Sigma}(y) &= \int \mathbf{x}\mathbf{x}^\top d\pi_{\mathbf{x}|y}(\mathbf{x}) - \boldsymbol{\mu}(y)\boldsymbol{\mu}(y)^\top \\ &= \begin{bmatrix} \alpha(y) & 0 \\ 0 & y^2 - \sqrt{2}y + \frac{3}{2} \end{bmatrix} - \begin{bmatrix} 0 \\ y - \frac{1}{\sqrt{2}} \end{bmatrix} \begin{bmatrix} 0 & y - \frac{1}{\sqrt{2}} \end{bmatrix} \\ &= \begin{bmatrix} \alpha(y) & 0 \\ 0 & 1 \end{bmatrix}. \end{aligned}$$

Let $\mathbf{b} = [0, 1]^\top$ and note

$$(4.22) \quad \boldsymbol{\Sigma}(y)\mathbf{b} = \begin{bmatrix} \alpha(y) & 0 \\ 0 & 1 \end{bmatrix} \begin{bmatrix} 0 \\ 1 \end{bmatrix} = \begin{bmatrix} 0 \\ 1 \end{bmatrix} = \mathbf{b},$$

for all y . From (4.18), $\mathbf{b} \in \text{null}(\mathbf{C}_{\text{AVE}})$ which implies that \mathbf{C}_{AVE} is rank-one. However, the central subspace of f is \mathbb{R}^2 . Hence, $\text{colspan}(\mathbf{C}_{\text{AVE}}) \subset \mathcal{S}_{f, \pi_{\mathbf{x}}}$.

In Example 2, \mathbf{C}_{AVE} would suggest that we disregard x_2 for dimension reduction, but f depends on x_2 . It is important to be aware of and understand the potential for misleading results from the subspaces of \mathbf{C}_{AVE} (and \mathbf{C}_{IR}) when working with deterministic functions.

The second limitation of \mathbf{C}_{AVE} arises from the elliptic symmetry requirement on the input density $p_{\mathbf{x}}$. When $p_{\mathbf{x}}$ is not elliptically symmetric, we cannot guarantee that the column space of \mathbf{C}_{AVE} is contained within the central subspace. Thus, a basis for the column space of \mathbf{C}_{AVE} could be contaminated by effects of $\pi_{\mathbf{x}}$ —independent of whether or not f is a ridge function.

Next we consider the sliced version of \mathbf{C}_{AVE} . We use the same slicing function h from (2.9) to approximate \mathbf{C}_{AVE} from (4.17). The sliced approximation of \mathbf{C}_{AVE} is

$$(4.23) \quad \mathbf{C}_{\text{SAVE}} = \sum_{r=1}^R \omega(r) (\mathbf{I} - \boldsymbol{\Sigma}_h(r))^2,$$

where $\omega(r)$ is the probability mass function from (4.7) and

$$(4.24) \quad \boldsymbol{\Sigma}_h(r) = \int (\mathbf{x} - \boldsymbol{\mu}_h(r)) (\mathbf{x} - \boldsymbol{\mu}_h(r))^\top d\pi_{\mathbf{x}|r}(\mathbf{x}).$$

By containment of the central subspace,

$$(4.25) \quad \text{colspan}(\mathbf{C}_{\text{SAVE}}) \subseteq \mathcal{S}_{h \circ f, \pi_{\mathbf{x}}} \subseteq \mathcal{S}_{f, \pi_{\mathbf{x}}}.$$

We can interpret \mathbf{C}_{SAVE} as a Riemann sum approximation of \mathbf{C}_{AVE} using a similar argument as in Section 4.1. An important corollary of (4.25) is that the rank of \mathbf{C}_{SAVE} is bounded above by the dimension of f 's central subspace.

Algorithm 2.2 computes a sample approximation of \mathbf{C}_{SAVE} , denoted $\hat{\mathbf{C}}_{\text{SAVE}}$, using given input/output pairs $\{[\mathbf{x}_i^\top, y_i]\}$. When the \mathbf{x}_i are sampled independently according to $\pi_{\mathbf{x}}$ and each $y_i = f(\mathbf{x}_i)$ is a deterministic function query, we can interpret $\hat{\mathbf{C}}_{\text{SAVE}}$ as a Monte Carlo approximation to \mathbf{C}_{SAVE} . Thus, $\hat{\mathbf{C}}_{\text{SAVE}}$ and its eigenpairs are random—not because of any randomness in the map f but because of the random choices of \mathbf{x}_i . The following theorem shows the rate of mean-squared convergence of the eigenvalues of $\hat{\mathbf{C}}_{\text{SAVE}}$.

THEOREM 4.6. *Assume that Algorithm 2.2 has been applied to the data set $\{[\mathbf{x}_i^\top, y_i]\}$, with $i = 1, \dots, N$, where the \mathbf{x}_i are drawn independently according to $\pi_{\mathbf{x}}$ and $y_i = f(\mathbf{x}_i)$ are point evaluations of f . Then, for $k = 1, \dots, m$,*

$$(4.26) \quad \mathbb{E} \left[\left(\lambda_k(\mathbf{C}_{\text{SAVE}}) - \lambda_k(\hat{\mathbf{C}}_{\text{SAVE}}) \right)^2 \right] = \mathcal{O}(N_{r_{\min}}^{-1})$$

where $\lambda_k(\cdot)$ denotes the k th eigenvalue of the given matrix.

The proof is in Appendix A.6. We note that the column space of $\hat{\mathbf{C}}_{\text{SAVE}}$ is not contained in f 's central subspace because of finite sampling. However, using a sequence of estimates with increasing N , one may be able to distinguish effects of finite sampling from true directions of variability in f .

Next, we examine the convergence of the subspaces Algorithm 2.2 produces, where the subspace distance is from (4.14).

THEOREM 4.7. *Assume the same conditions from Theorem 4.6. Then, for sufficiently large N ,*

$$(4.27) \quad \text{dist} \left(\text{colspan}(\mathbf{A}), \text{colspan}(\hat{\mathbf{A}}) \right) = \frac{1}{\lambda_n(\mathbf{C}_{\text{SAVE}}) - \lambda_{n+1}(\mathbf{C}_{\text{SAVE}})} \mathcal{O}_p(N_{r_{\min}}^{-1/2}).$$

The proof is in Appendix A.7. The subspace error for Algorithm 2.2 decays asymptotically like $N_{r_{\min}}^{-1/2}$ with high probability. Similar to the estimated SIR subspace from Algorithm 2.1, the error depends inversely on the eigenvalue gap. If the gap between the n th and $(n+1)$ th eigenvalues is large, then the error in the estimated n -dimensional subspace is small for a fixed number of samples.

5. Numerical results. We apply SIR and SAVE to three ridge functions to study the methods' applicability for ridge recovery and verify our convergence analysis. Since we are not concerned with using SIR and SAVE for ridge approximation, we do not study the methods' behavior for functions that are not ridge functions. For each ridge function, we provide several graphics including convergence plots of estimated eigenvalues, eigenvalue errors, and subspace errors. One graphic is especially useful for visualizing the structure of the function relative to its central subspace: the sufficient summary plot [14]. Sufficient summary plots show y versus $\mathbf{A}^\top \mathbf{x}$, where \mathbf{A} has only one or two columns that comprise a basis for the central subspace. Algorithms 2.1 and 2.2 produce eigenvectors that span an approximation of the SIR and SAVE subspaces, respectively. We use these eigenvectors to construct the low-dimensional inputs for

sufficient summary plots. The label *sufficient* is tied to the precise definition of statistical sufficiency in sufficient dimension reduction for regression.

The convergence analysis from sections 4.1 and 4.2 assume a fixed slicing of the observed y range. However, Algorithms 2.1 and 2.2 are implemented using an adaptive slicing approach that attempts to maximize $N_{r_{\min}}$ for a given set of data. This is done as a heuristic technique for reducing eigenvalue and subspace errors.

The python code used to generate the figures is available at <https://bitbucket.org/aglaws/inverse-regression-for-ridge-recovery>. The scripts require the dev branch of the Python Active-subspaces Utility Library, <https://github.com/paulcon/active-subspaces/tree/dev>.

5.1. One-dimensional quadratic ridge function. We study a simple one-dimensional quadratic ridge function to contrast the recovery properties of SIR versus SAVE. Let $\pi_{\mathbf{x}}$ have a standard multivariate Gaussian density function on \mathbb{R}^{10} . Define

$$(5.1) \quad y = f(\mathbf{x}) = (\mathbf{b}^\top \mathbf{x})^2,$$

where $\mathbf{b} \in \mathbb{R}^{10}$ is a constant vector. The span of \mathbf{b} is the central subspace. First, we attempt to estimate the central subspace using SIR (Algorithm 2.1), which is known to fail for functions symmetric about $\mathbf{x} = \mathbf{0}$ [17]; Figure 1 confirms this failure. In fact, \mathbf{C}_{IR} is zero since the conditional expectation of \mathbf{x} for any value of y is zero. Figure 1a shows that all estimated eigenvalues of the SIR matrix are nearly zero as expected. Figure 1b is a one-dimensional sufficient summary plot of y_i against $\hat{\mathbf{w}}_1^\top \mathbf{x}_i$, where $\hat{\mathbf{w}}_1$ denotes the normalized eigenvector associated with the largest eigenvalue of $\hat{\mathbf{C}}_{\text{SIR}}$ from Algorithm 2.1. If (i) the central subspace is one-dimensional (as in this case) and (ii) the chosen SDR algorithm correctly identifies the one basis vector, then the sufficient summary plot will show a univariate relationship between the linear combination of input evaluations and the associated outputs. Due to the symmetry in the quadratic function, SIR fails to recover the basis vector; the sufficient summary plot's lack of univariate relationship confirms the failure.

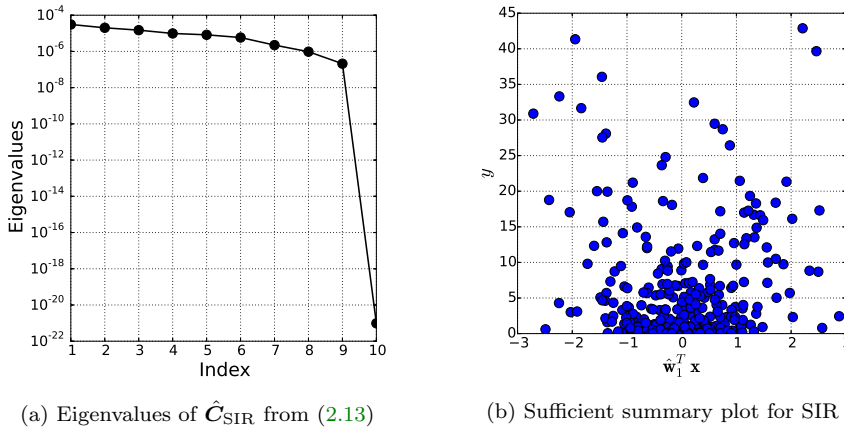


Fig. 1: As expected, SIR fails to recover the ridge direction \mathbf{b} in the function (5.1).

Figure 2 shows results from applying SAVE (Algorithm 2.2) to the quadratic function (5.1). Figure 2a shows the eigenvalues of $\hat{\mathbf{C}}_{\text{SAVE}}$ from Algorithm 2.2. Note

the large gap between the first and second eigenvalues, which suggests that the SAVE subspace is one-dimensional. Figure 2b shows the sufficient summary plot using the first eigenvector $\hat{\mathbf{w}}_1$ from Algorithm 2.2, which reveals the univariate quadratic relationship between $\hat{\mathbf{w}}_1^\top \mathbf{x}$ and y .

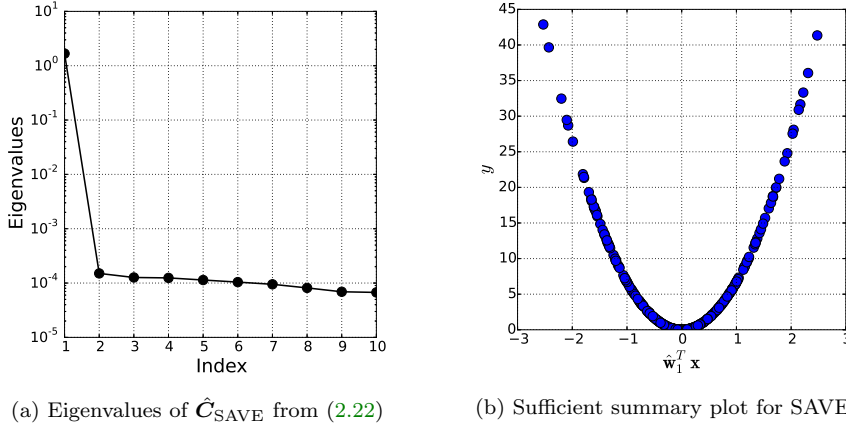


Fig. 2: SAVE recovers the ridge direction \mathbf{b} in the function (5.1).

5.2. Three-dimensional quadratic function. Next, we numerically study the convergence properties of the SIR and SAVE algorithms using a more complex quadratic function. Let $\pi_{\mathbf{x}}$ have a standard multivariate Gaussian density function on \mathbb{R}^{10} . Define

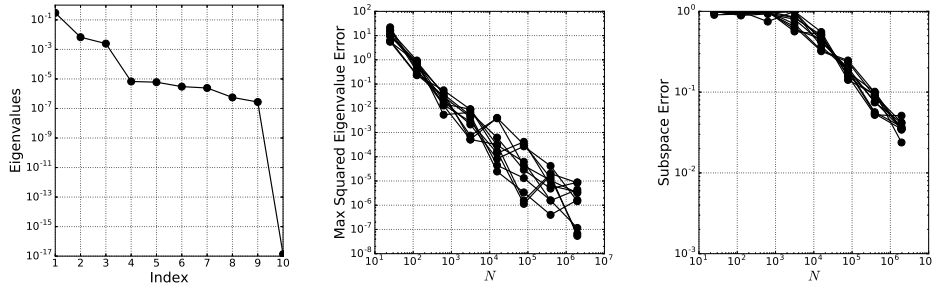
$$(5.2) \quad y = f(\mathbf{x}) = \mathbf{x}^\top \mathbf{B} \mathbf{B}^\top \mathbf{x} + \mathbf{b}^\top \mathbf{x},$$

where $\mathbf{B} \in \mathbb{R}^{10 \times 2}$ and $\mathbf{b} \in \mathbb{R}^{10}$ with $\mathbf{b} \notin \text{colspan}(\mathbf{B})$. Figure 3a shows the eigenvalues of $\hat{\mathbf{C}}_{\text{SIR}}$; note the gap between the third and fourth eigenvalues. Figure 3b shows the maximum squared eigenvalue error normalized by the largest eigenvalue,

$$(5.3) \quad \max_{1 \leq i \leq m} \frac{\left(\lambda_i(\hat{\mathbf{C}}_{\text{SIR}}) - \lambda_i(\mathbf{C}_{\text{SIR}}) \right)^2}{\lambda_1(\mathbf{C}_{\text{SIR}})^2},$$

for increasing numbers of samples in 10 independent trials. We estimate the true eigenvalues using SIR with 10^7 samples. The average error decays at a rate slightly faster than the $\mathcal{O}(N^{-1})$ from Theorem 4.3. The improvement can likely be attributed to the adaptive slicing procedure discussed at the beginning of this section. Figure 3c shows the error in the estimated three-dimensional SIR subspace (see (4.14)) for increasing numbers of samples. We use 10^7 samples to estimate the true SIR subspace. The subspace errors decrease asymptotically at a rate of approximately $\mathcal{O}(N^{-1/2})$, which agrees with Theorem 4.4.

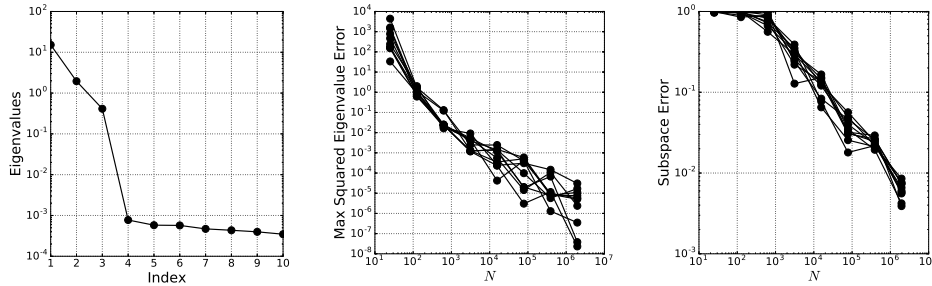
Figure 4 shows the results of a similar convergence study using SAVE (Algorithm 2.2). The eigenvalues of $\hat{\mathbf{C}}_{\text{SAVE}}$ from (2.22) are shown in Figure 4a. Note the large gap between the third and fourth eigenvalues, which is consistent with the three-dimensional central subspace in f from (5.2). Figures 4b and 4c show the maximum



(a) Eigenvalues of \hat{C}_{SIR} from (b) Maximum squared eigen- (c) SIR subspace errors for $n =$
(2.13) value error, SIR 3

Fig. 3: Eigenvalues, eigenvalue errors, and subspace errors for SIR applied to (5.2). The error decreases with increasing samples consistent with the convergence theory in section 4.1.

squared eigenvalue error and the subspace error, respectively, for $n = 3$. The eigenvalue error again decays at a faster rate than expected in Theorem 4.6—likely due to the adaptive slicing implemented in the code. The subspace error decays consistently according to Theorem 4.7.



(a) Eigenvalues of \hat{C}_{SAVE} from (b) Maximum squared eigen- (c) SAVE subspace errors for
(2.22) value error, SAVE $n = 3$

Fig. 4: Eigenvalues, eigenvalue errors, and subspace errors for SAVE applied to (5.2). The error decreases with increasing samples consistent with the convergence theory in section 4.2.

5.3. Hartmann problem. The following study steps in the direction of using SIR and SAVE for parameter space dimension reduction in a physics-based model. The Hartmann problem is a standard problem in magnetohydrodynamics (MHD) that models the flow of an electrically-charged plasma in the presence of a uniform magnetic field [18]. The flow occurs along an infinite channel between two parallel plates separated by distance 2ℓ . The applied magnetic field is perpendicular to the flow direction and acts as a resistive force on the flow velocity. At the same time, the movement of the fluid induces a magnetic field along the direction of the flow. Figure

5 contains a diagram of this problem. We have recently used the following model as a test case for parameter space dimension reduction methods [28].

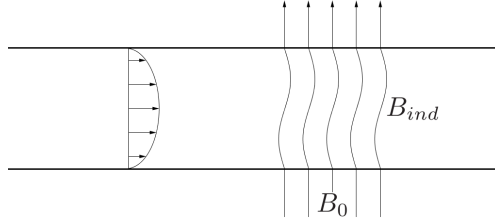


Fig. 5: The Hartmann problem studies the flow of an ionized fluid between two parallel plates. A magnetic field applied perpendicular to the flow direction acts as a resistive force to the fluid flow. Simultaneously, the fluid induces a magnetic field along the direction of the flow.

The inputs to the Hartmann model are fluid viscosity μ , fluid density ρ , applied pressure gradient $\partial p_0/\partial x$ (where the derivative is with respect to the flow field's spatial coordinate), resistivity η , and applied magnetic field B_0 . We collect these inputs into a vector,

$$(5.4) \quad \mathbf{x} = [\mu \quad \rho \quad \frac{\partial p_0}{\partial x} \quad \eta \quad B_0]^\top.$$

The output of interest is the total induced magnetic field,

$$(5.5) \quad B_{ind}(\mathbf{x}) = \frac{\partial p_0}{\partial x} \frac{\ell \mu_0}{2B_0} \left(1 - 2 \frac{\sqrt{\eta \mu}}{B_0 \ell} \tanh \left(\frac{B_0 \ell}{2\sqrt{\eta \mu}} \right) \right).$$

This function is not a ridge function of \mathbf{x} . However, it has been shown that many physical laws can be expressed as ridge functions by considering a log transform of the inputs, which relates ridge structure in the function to dimension reduction via the Buckingham Pi Theorem [8]. For this reason, we apply SIR and SAVE ridge recovery to B_{ind} as a function of the logarithms of the inputs from (5.4). The log-transformed inputs are equipped with a multivariate Gaussian with mean $\boldsymbol{\mu}$ and covariance $\boldsymbol{\Sigma}$,

$$(5.6) \quad \boldsymbol{\mu} = \begin{bmatrix} -2.25 \\ 1 \\ 0.3 \\ 0.3 \\ -0.75 \end{bmatrix}, \quad \boldsymbol{\Sigma} = \begin{bmatrix} 0.15 & & & & \\ & 0.25 & & & \\ & & 0.25 & & \\ & & & 0.25 & \\ & & & & 0.25 \end{bmatrix}.$$

Figure 6 shows the results of applying SIR (Algorithm 2.1) to the Hartmann model for the induced magnetic field B_{ind} . The eigenvalues of \hat{C}_{SIR} from (2.13) with bootstrap ranges are shown in Figure 6a. Large gaps appear after the first and second eigenvalues, which indicates possible two-dimensional ridge structure. In fact, the induced magnetic field admits a two-dimensional central subspace relative to the log-inputs [28]. Figures 6c and 6d contain one- and two-dimensional sufficient summary plots of B_{ind} against $\hat{\mathbf{w}}_1^\top \mathbf{x}$ and $\hat{\mathbf{w}}_2^\top \mathbf{x}$, where $\hat{\mathbf{w}}_1$ and $\hat{\mathbf{w}}_2$ are the first two eigenvectors of \hat{C}_{SIR} . We see a strong one-dimensional relationship. However, the two-dimensional sufficient summary plot shows slight curvature with changes in $\hat{\mathbf{w}}_2^\top \mathbf{x}$. These results

suggest that ridge-like structure may be discovered using the SIR algorithm in some cases. Figure 6b shows the subspace errors as a function of the subspace dimension. Recall from Theorem 4.4 that the subspace error depends inversely on the eigenvalue gap. The largest eigenvalue gap occurs between the first and second eigenvalues, which is consistent with the smallest subspace error for $n = 1$.

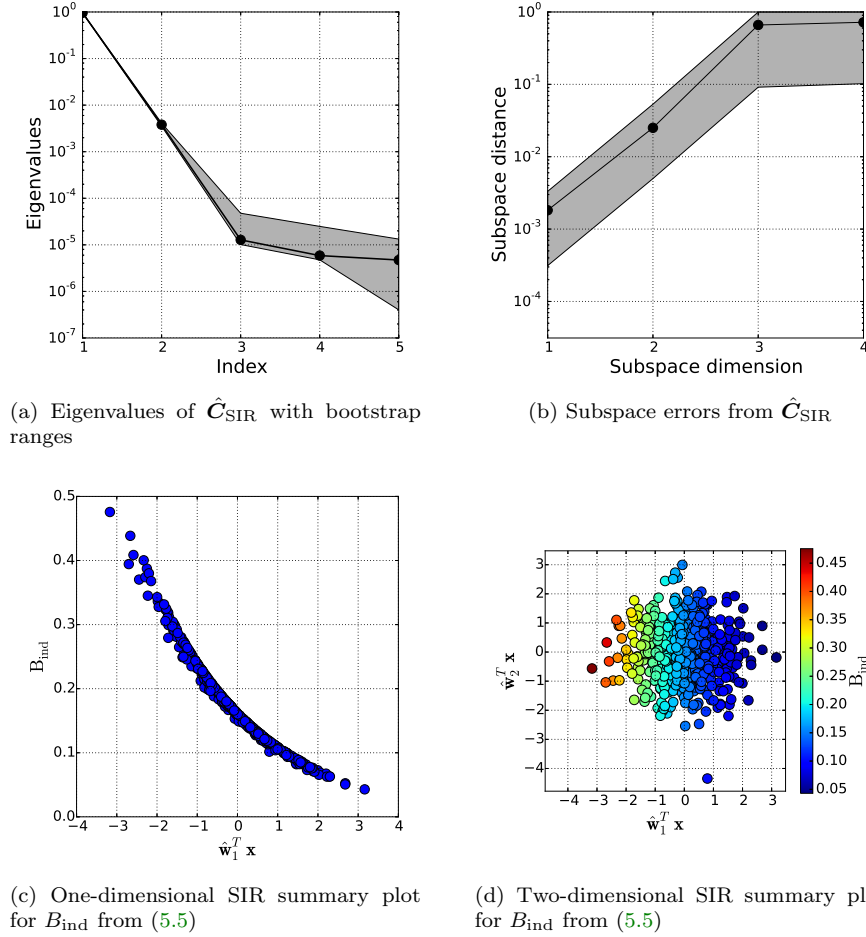


Fig. 6: Eigenvalues with bootstrap ranges, estimated subspace errors, and sufficient summary plots for SIR (Algorithm 2.1) applied to B_{ind} from (5.5).

We perform the same numerical studies using SAVE. Figure 7a shows the eigenvalues of the \hat{C}_{SAVE} from (2.22) for the induced magnetic field B_{ind} from (5.5). Note the large gaps after the first and second eigenvalues. These gaps are consistent with the subspace errors in Figure 7b, where the one- and two-dimensional subspace estimates have the smallest errors. Figures 7c and 7d contain sufficient summary plots for $\hat{w}_1^\top x$ and $\hat{w}_2^\top x$, where \hat{w}_1 and \hat{w}_2 are the first two eigenvectors from \hat{C}_{SAVE} in (2.22).

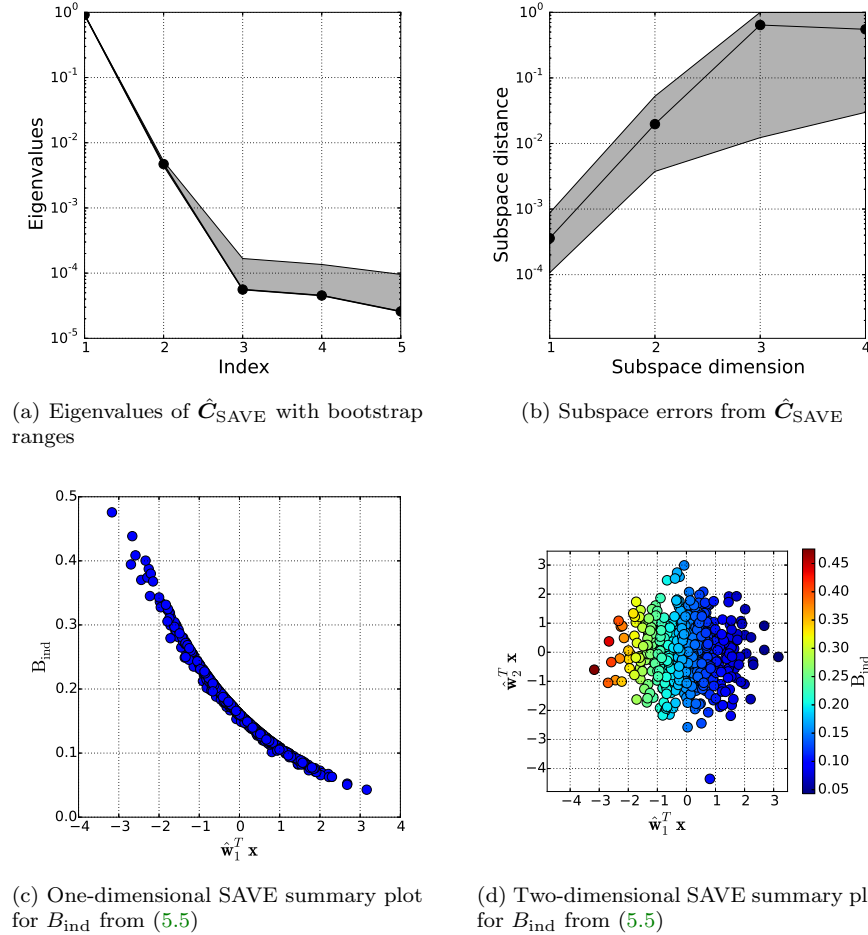


Fig. 7: Eigenvalues with bootstrap ranges, estimated subspace errors, and sufficient summary plots for SAVE (Algorithm 2.2) applied to B_{ind} from (5.5).

6. Summary and conclusion. Seeking data-driven machine learning methods for computational science models, we investigate sufficient dimension reduction from statistical regression as a tool for subspace-based input space dimension reduction in deterministic functions. We show that SDR is theoretically justified as a tool for ridge recovery by proving equivalence of the dimension reduction subspace and the ridge subspace for some deterministic $y = f(\mathbf{x})$. We interpret two SDR algorithms for the ridge recovery problem: sliced inverse regression and sliced average variance estimation. In regression, these methods use moments of the inverse regression $\mathbf{x}|y$ to estimate subspaces relating to the central subspace. In ridge recovery, we reinterpret SIR and SAVE as numerical integration methods for estimating inverse conditional moment matrices, where the integrals are over contour sets of f . We show that the column spaces of the conditional moment matrices are contained in the ridge subspace,

which justifies their eigenspaces as tools ridge recovery.

Appendix A. Proofs.

In what follows, we prove the various theorems presented in Section 4. We begin by introducing a lemma that will simplify this task. This lemma enables quick analysis of the asymptotic behavior of multiple summations over complicated multi-index sets. Define the multi-index set

$$(A.1) \quad \mathcal{K}^{p,q}(r) = \left\{ \mathbf{k} \in \mathbb{N}^{p+q} \left| \begin{array}{l} k_1, \dots, k_p \in \{1, \dots, N\} \\ \text{and } k_{p+1}, \dots, k_{p+q} \in \{1, \dots, N_r\} \end{array} \right. \right\}$$

where $N_r \leq N$. Let $\mathbf{b} \in \mathbb{R}^{p+q}$ be a random vector and let $\{\mathbf{b}^k\}$, $k = 1, \dots, N$, denote N independent realizations of \mathbf{b} where N is from (A.1). Define the $(p+q)$ -dimensional tensor $\mathbf{B}^{p,q}(r)$ whose elements are given by

$$(A.2) \quad B_{\mathbf{k}}^{p,q}(r) = \mathbb{E} \left[b_1^{k_1} \dots b_p^{k_p} b_{p+1}^{k_{p+1}} \dots b_{p+q}^{k_{p+q}} \right]$$

for $\mathbf{k} \in \mathcal{K}^{p,q}(r)$. Note that the k_i 's above do not indicate powers of b_j , but rather indices. That is, $b_j^{k_i}$ denotes the j th entry of \mathbf{b}^k which is the k th realization of the random vector \mathbf{b} . Thus,

$$(A.3) \quad \mathbf{B}^{p,q}(r) \in \mathbb{R}^{\overbrace{N \times \dots \times N}^p \times \overbrace{N_r \times \dots \times N_r}^q}.$$

The following lemma plays an important role in upcoming proofs.

LEMMA A.1. *Let $\mathbf{b} \in \mathbb{R}^{p+q}$ be a random vector and let $\{\mathbf{b}^k\}$, $k = 1, \dots, N$, denote N independent realizations of \mathbf{b} . Define $N_r \in \mathbb{N}$ such that $p+q \leq N_r \leq N$. Let $\mathcal{K}^{p,q}(r)$ and $\mathbf{B}^{p,q}(r)$ be defined according to (A.1) and (A.2), respectively. Then,*

$$(A.4) \quad \sum_{\mathbf{k} \in \mathcal{K}^{p,q}(r)} B_{\mathbf{k}}^{p,q}(r) = N^p N_r^q \mathbb{E}[b_1] \dots \mathbb{E}[b_p] \mathbb{E}[b_{p+1}] \dots \mathbb{E}[b_{p+q}] \\ + \mathcal{O}(N^p N_r^{q-1} + N^{p-1} N_r^q).$$

Proof. Define the following subsets of $\mathcal{K}^{p,q}(r)$:

$$(A.5) \quad \mathcal{K}_1^{p,q}(r) = \{ \mathbf{k} \in \mathcal{K}^{p,q}(r) \mid k_i \neq k_j \text{ for } i, j = 1, \dots, p+q \text{ and } i \neq j \}, \\ \mathcal{K}_2^{p,q}(r) = \mathcal{K}^{p,q}(r) \setminus \mathcal{K}_1^{p,q}(r).$$

Asymptotically, the subset $\mathcal{K}_1^{p,q}(r)$ has

$$(A.6) \quad \left(\prod_{i=0}^{q-1} (N_r - i) \right) \left(\prod_{j=q}^{p+q-1} (N - j) \right) = N^p N_r^q + \mathcal{O}(N^p N_r^{q-1} + N^{p-1} N_r^q)$$

elements. Since all of the indices are unique for any $\mathbf{k} \in \mathcal{K}_1^{p,q}(r)$,

$$(A.7) \quad B_{\mathbf{k}}^{p,q}(r) = \mathbb{E}[b_1] \dots \mathbb{E}[b_p] \mathbb{E}[b_{p+1}] \dots \mathbb{E}[b_{p+q}].$$

Consider the number of elements in $\mathcal{K}_2^{p,q}(r)$. By construction, any $\mathbf{k} \in \mathcal{K}_2^{p,q}(r)$ must have at least two identical indices. As N and N_r tend towards infinity, the largest subset of elements in $\mathcal{K}_2^{p,q}(r)$ will be those with only two identical elements. There are three such cases:

Case 1:

Two of the k_i 's which range from $1, \dots, N$ are identical and all other k_i 's are unique. There are

$$(A.8) \quad \left(\prod_{i=0}^{q-1} (N_r - i) \right) \left(\prod_{j=q}^{p+q-2} (N - j) \right) = \mathcal{O}(N^{p-1} N_r^q)$$

such elements.

Case 2:

Two of the k_i 's which range from $1, \dots, N_r$ are identical and all other k_i 's are unique. There are

$$(A.9) \quad \left(\prod_{i=0}^{q-2} (N_r - i) \right) \left(\prod_{j=q-1}^{p+q-2} (N - j) \right) = \mathcal{O}(N^p N_r^{q-1})$$

such elements.

Case 3:

One k_i which range from $1, \dots, N$ and one k_i which ranges from $1, \dots, N_r$ are identical and all other k_i 's are unique. There are

$$(A.10) \quad \left(\prod_{i=0}^{q-1} (N_r - i) \right) \left(\prod_{j=q}^{p+q-2} (N - j) \right) = \mathcal{O}(N^{p-1} N_r^q)$$

such elements. Thus, there are $\mathcal{O}(N^p N_r^{q-1} + N^{p-1} N_r^q)$ elements in $\mathcal{K}_2^{p,q}(r)$.

Therefore,

$$(A.11) \quad \sum_{\mathbf{k} \in \mathcal{K}^{p,q}(r)} B_{\mathbf{k}}^{p,q}(r) = \sum_{\mathbf{k} \in \mathcal{K}_1^{p,q}(r)} B_{\mathbf{k}}^{p,q}(r) + \sum_{\mathbf{k} \in \mathcal{K}_2^{p,q}(r)} B_{\mathbf{k}}^{p,q}(r) \\ = (N^p N_r^q + \mathcal{O}(N^p N_r^{q-1} + N^{p-1} N_r^q)) \mathbb{E}[b_1] \dots \mathbb{E}[b_p] \mathbb{E}[b_{p+1}] \dots \mathbb{E}[b_{p+q}] \\ + \mathcal{O}(N^p N_r^{q-1} + N^{p-1} N_r^q) \\ = N^p N_r^q \mathbb{E}[b_1] \dots \mathbb{E}[b_p] \mathbb{E}[b_{p+1}] \dots \mathbb{E}[b_{p+q}] + \mathcal{O}(N^p N_r^{q-1} + N^{p-1} N_r^q)$$

A.1. Proof of Theorem 4.1.

THEOREM 4.1. *Let (Ω, Σ, P) be a probability triple. Suppose that $\mathbf{x} : \Omega \rightarrow \mathbb{R}^m$ and $y : \Omega \rightarrow \mathbb{R}$ are random variables related by a measurable function $f : \mathbb{R}^m \rightarrow \mathbb{R}$ so that $y = f(\mathbf{x})$. Let $\mathbf{A} \in \mathbb{R}^{m \times n}$ be a constant matrix. Then $y \perp\!\!\!\perp \mathbf{x} | \mathbf{A}^\top \mathbf{x}$ if and only if $y = g(\mathbf{A}^\top \mathbf{x})$ where $g : \mathbb{R}^n \rightarrow \mathbb{R}$ is a measurable function.*

Proof. Assume that $y = f(\mathbf{x}) = g(\mathbf{A}^\top \mathbf{x})$ for some \mathbf{A} and g , then conditional independence follows since the value of $\mathbf{A}^\top \mathbf{x}$ fully determines y .

Next, assume that $y \perp\!\!\!\perp \mathbf{x} | \mathbf{A}^\top \mathbf{x}$, and note that $\mathbf{A}^\top \mathbf{x} : \Omega \rightarrow \mathbb{R}^n$ is a random vector. Consider conditional dependence in terms of the generated σ -algebras,

$$(A.12) \quad \sigma(y) \perp\!\!\!\perp \sigma(\mathbf{x}) | \sigma(\mathbf{A}^\top \mathbf{x})$$

where

$$(A.13) \quad \begin{aligned} \sigma(y) &= \{y^{-1}(B) : B \in \mathcal{B}(\mathbb{R})\}, \\ \sigma(\mathbf{x}) &= \{\mathbf{x}^{-1}(B) : B \in \mathcal{B}(\mathbb{R}^m)\}, \\ \sigma(\mathbf{A}^\top \mathbf{x}) &= \{(\mathbf{A}^\top \mathbf{x})^{-1}(B) : B \in \mathcal{B}(\mathbb{R}^n)\}, \end{aligned}$$

and $\mathcal{B}(\cdot)$ is the Borel σ -algebra over the indicated domain. By (A.12),

$$(A.14) \quad \mathbb{E}[z | \sigma(\mathbf{A}^\top \mathbf{x})] = \mathbb{E}[z | \sigma(\sigma(\mathbf{A}^\top \mathbf{x}) \cup \sigma(\mathbf{x}))]$$

where $z : \Omega \rightarrow \mathbb{R}^+$ is any $\sigma(y)$ -measurable random variable [45, Proposition 13, Chapter 3].

Define the partition $y = y^+ - y^-$ where

$$(A.15) \quad \begin{aligned} y^+ &= f^+(\mathbf{x}) = \begin{cases} f(\mathbf{x}) & \text{if } f(\mathbf{x}) > 0 \\ 0 & \text{otherwise} \end{cases}, \\ y^- &= f^-(\mathbf{x}) = \begin{cases} -f(\mathbf{x}) & \text{if } f(\mathbf{x}) < 0 \\ 0 & \text{otherwise} \end{cases}. \end{aligned}$$

Since y is measurable, $y^+ : \Omega \rightarrow \mathbb{R}^+$ is $\sigma(y)$ -measurable [57]. Applying (A.14) to y^+ ,

$$(A.16) \quad \mathbb{E}[y^+ | \sigma(\mathbf{A}^\top \mathbf{x})] = \mathbb{E}[y^+ | \sigma(\sigma(\mathbf{A}^\top \mathbf{x}) \cup \sigma(\mathbf{x}))].$$

The transformation $\mathbf{A}^\top \mathbf{x}$ is $\mathcal{B}(\mathbb{R}^n)$ -measurable since it is linear. Therefore, $\sigma(\mathbf{A}^\top \mathbf{x}) \subseteq \sigma(\mathbf{x})$, and (A.16) becomes

$$(A.17) \quad \mathbb{E}[y^+ | \sigma(\mathbf{A}^\top \mathbf{x})] = \mathbb{E}[y^+ | \sigma(\mathbf{x})].$$

By the Doob-Dynkin Lemma [45, Proposition 3, Chapter 1], y^+ is $\sigma(\mathbf{x})$ -measurable since $y^+ = f^+(\mathbf{x})$. Combining this with (A.17),

$$(A.18) \quad y^+ = f^+(\mathbf{x}) = \mathbb{E}[y^+ | \sigma(\mathbf{x})] = \mathbb{E}[y^+ | \sigma(\mathbf{A}^\top \mathbf{x})].$$

This argument also applies for $y^- : \Omega \rightarrow \mathbb{R}^+$ such that

$$(A.19) \quad y^- = f^-(\mathbf{x}) = \mathbb{E}[y^- | \sigma(\mathbf{x})] = \mathbb{E}[y^- | \sigma(\mathbf{A}^\top \mathbf{x})].$$

Thus,

$$(A.20) \quad \begin{aligned} y &= y^+ - y^- \\ &= \mathbb{E}[y^+ | \sigma(\mathbf{A}^\top \mathbf{x})] - \mathbb{E}[y^- | \sigma(\mathbf{A}^\top \mathbf{x})] \\ &= \mathbb{E}[y^+ - y^- | \sigma(\mathbf{A}^\top \mathbf{x})] \\ &= \mathbb{E}[y | \sigma(\mathbf{A}^\top \mathbf{x})]. \end{aligned}$$

Therefore, y is $\sigma(\mathbf{A}^\top \mathbf{x})$ -measurable, and by the Doob-Dynkin Lemma [45, Proposition 3, Chapter 1], is a function of $\mathbf{A}^\top \mathbf{x}$. That is,

$$(A.21) \quad y = g(\mathbf{A}^\top \mathbf{x})$$

where $g : \mathbb{R}^n \rightarrow \mathbb{R}$ is a deterministic measurable function. \square

A.2. Proof of Theorem 4.2.

THEOREM 4.2. *Let $f : \mathbb{R}^m \rightarrow \mathbb{R}$ with input probability measure $\pi_{\mathbf{x}}$ admit a central subspace $\mathcal{S}_{f, \pi_{\mathbf{x}}}$, and assume $\pi_{\mathbf{x}}$ admits an elliptically symmetric and standardized density function. Then, $\text{colspan}(\mathbf{C}_{\text{IR}}) \subseteq \mathcal{S}_{f, \pi_{\mathbf{x}}}$.*

Proof. Consider the orthogonal $m \times m$ matrix $\begin{bmatrix} \mathbf{A} & \mathbf{B} \end{bmatrix}$ where $\mathbf{A} \in \mathbb{R}^{m \times n}$ and $\mathbf{B} \in \mathbb{R}^{m \times (m-n)}$ contain bases for $\mathcal{S}_{f, \pi_{\mathbf{x}}}$ and the orthogonal complement of $\mathcal{S}_{f, \pi_{\mathbf{x}}}$, respectively. Decompose \mathbf{x} into

$$(A.22) \quad \mathbf{x} = \mathbf{A}\mathbf{u} + \mathbf{B}\mathbf{v}$$

where $\mathbf{u} = \mathbf{A}^\top \mathbf{x} \in \mathbb{R}^n$ and $\mathbf{v} = \mathbf{B}^\top \mathbf{x} \in \mathbb{R}^{m-n}$.

Rewrite the conditional expectation in (4.4) as

$$(A.23) \quad \boldsymbol{\mu}(y) = \int \left[\int \mathbf{x} d\pi_{\mathbf{x}|\mathbf{u}}(\mathbf{x}) \right] d\pi_{\mathbf{u}|y}(\mathbf{u}),$$

where $\pi_{\mathbf{x}|\mathbf{u}}$ and $\pi_{\mathbf{u}|y}$ are the conditional probability measures over $\mathcal{X}(\mathbf{u}) = \{\mathbf{x} \in \mathbb{R}^m : \mathbf{u} = \mathbf{A}^\top \mathbf{x}\}$ and $g^{-1}(y) = \{\mathbf{u} \in \mathbb{R}^n : g(\mathbf{u}) = y\}$, respectively. By (A.22),

$$(A.24) \quad \mathcal{X}(\mathbf{u}) = \{\mathbf{x} \in \mathbb{R}^m \mid \mathbf{x} = \mathbf{A}\mathbf{u} + \mathbf{B}\mathbf{v}, \mathbf{v} \in \mathbb{R}^{m-n}\}.$$

Let $\pi_{\mathbf{v}|\mathbf{u}}$ denote the conditional probability measure induced by (A.22) and $\pi_{\mathbf{x}}$. Since \mathbf{x} is standardized with an elliptically symmetric density and $\begin{bmatrix} \mathbf{A} & \mathbf{B} \end{bmatrix}$ is an orthogonal matrix, $\pi_{\mathbf{v}|\mathbf{u}}$ is standardized and elliptically symmetric [33, Chapter 6]. Thus,

$$(A.25) \quad \begin{aligned} \int \mathbf{x} d\pi_{\mathbf{x}|\mathbf{u}}(\mathbf{x}) &= \int (\mathbf{A}\mathbf{u} + \mathbf{B}\mathbf{v}) d\pi_{\mathbf{v}|\mathbf{u}}(\mathbf{v}) \\ &= \mathbf{A}\mathbf{u} \int d\pi_{\mathbf{v}|\mathbf{u}}(\mathbf{v}) + \mathbf{B} \int \mathbf{v} d\pi_{\mathbf{v}|\mathbf{u}}(\mathbf{v}) \\ &= \mathbf{A}\mathbf{u} \end{aligned}$$

Combining (A.23) and (A.25),

$$(A.26) \quad \boldsymbol{\mu}(y) = \mathbf{A} \int \mathbf{u} d\mu_{\mathbf{u}|y}(\mathbf{u}).$$

Then, for $\mathbf{w} \in \text{null}(\mathbf{A}^\top)$,

$$(A.27) \quad \boldsymbol{\mu}(y)^\top \mathbf{w} = \left(\mathbf{A} \int \mathbf{u} d\mu_{\mathbf{u}|y}(\mathbf{u}) \right)^\top \mathbf{w} = \left(\int \mathbf{u}^\top d\mu_{\mathbf{u}|y}(\mathbf{u}) \right) (\mathbf{A}^\top \mathbf{w}) = 0.$$

By (4.5), $\mathbf{w}^\top \mathbf{C}_{\text{IR}} \mathbf{w} = 0$, which implies $\mathbf{w} \in \text{null}(\mathbf{C}_{\text{IR}})$. Therefore, $\text{null}(\mathbf{A}^\top) \subseteq \text{null}(\mathbf{C}_{\text{IR}})$, which implies

$$(A.28) \quad \text{colspan}(\mathbf{C}_{\text{IR}}) \subseteq \text{colspan}(\mathbf{A}) = \mathcal{S}_{f, \pi_{\mathbf{x}}}$$

as required. \square

A.3. Proof of Theorem 4.3.

THEOREM 4.3. *Assume that Algorithm 2.1 has been applied to the data set $\{[\mathbf{x}_i^\top, y_i]\}$, with $i = 1, \dots, N$, where the \mathbf{x}_i are drawn independently according to $\pi_{\mathbf{x}}$ and $y_i = f(\mathbf{x}_i)$ are point evaluations of f . Then, for $k = 1, \dots, m$,*

$$(4.13) \quad \mathbb{E} \left[\left(\lambda_k(\mathbf{C}_{\text{SIR}}) - \lambda_k(\tilde{\mathbf{C}}_{\text{SIR}}) \right)^2 \right] = \mathcal{O}(N_{r_{\min}}^{-1})$$

where $\lambda_k(\cdot)$ denotes the k th eigenvalue of the given matrix.

Proof. Recall the SIR matrix from (4.9),

$$(A.29) \quad \mathbf{C}_{\text{SIR}} = \sum_{r=1}^R \omega(r) \boldsymbol{\mu}_h(r) \boldsymbol{\mu}_h(r)^\top.$$

Algorithm 2.1 computes a sample approximation of \mathbf{C}_{SIR} ,

$$(A.30) \quad \hat{\mathbf{C}}_{\text{SIR}} = \sum_{r=1}^R \hat{\omega}(r) \hat{\boldsymbol{\mu}}_h(r) \hat{\boldsymbol{\mu}}_h(r)^\top$$

where

$$(A.31) \quad \hat{\omega}(r) = \frac{N_r}{N} \quad \text{and} \quad \hat{\boldsymbol{\mu}}_h(r) = \frac{1}{N_r} \sum_{i \in \mathcal{I}_r} \mathbf{x}_i$$

where \mathcal{I}_r is the set of indices for which $y_i \in J_r$ and N_r is the cardinality of \mathcal{I}_r . Rewrite $\hat{\omega}(r)$ as

$$(A.32) \quad \hat{\omega}(r) = \frac{1}{N} \sum_{i=1}^N \chi(y_i \in J_r)$$

where $\chi(y_i \in J_r)$ is an indicator function that is 1 when $y_i \in J_r$ and 0 otherwise.

Fix r and let

$$(A.33) \quad \omega = \omega(r), \quad \hat{\omega} = \hat{\omega}(r), \quad \chi_i = \chi(y_i \in J_r), \quad \boldsymbol{\mu} = \boldsymbol{\mu}_h(r), \quad \hat{\boldsymbol{\mu}} = \hat{\boldsymbol{\mu}}_h(r)$$

for convenience. Assume without loss of generality that $\mathcal{I}_r = \{1, \dots, N_r\}$.

To compute the mean squared error, we focus on the computation of a single element in $\hat{\mathbf{C}}_{\text{SIR}}$. To do this, we move the sample index to the superscript and let the subscript denote the vector or matrix element. That is, we let \hat{x}_i^k denote the i th element of the vector $\hat{\mathbf{x}}^k$ which is the k th realization of the random vector \mathbf{x} .

For $1 \leq i, j \leq m$,

$$(A.34) \quad \begin{aligned} \mathbb{E}[\hat{\omega} \hat{\mu}_i \hat{\mu}_j] &= \mathbb{E} \left[\left(\frac{1}{N} \sum_{k_1=1}^N \chi^{k_1} \right) \left(\frac{1}{N_r} \sum_{k_2=1}^{N_r} x_i^{k_2} \right) \left(\frac{1}{N_r} \sum_{k_3=1}^{N_r} x_j^{k_3} \right) \right] \\ &= \frac{1}{N N_r^2} \sum_{k_1=1}^N \sum_{k_2, k_3=1}^{N_r} \mathbb{E}[\chi^{k_1} x_i^{k_2} x_j^{k_3}]. \end{aligned}$$

Using (A.1) and (A.2), write

$$(A.35) \quad \mathbb{E}[\hat{\omega} \hat{\mu}_i \hat{\mu}_j] = \frac{1}{N N_r^2} \sum_{\mathbf{k} \in \mathcal{K}^{1,2}} B_{\mathbf{k}}^{1,2}.$$

Note that we drop the argument from $\mathcal{K}_{\mathbf{k}}^{1,2}(r)$ and $B_{\mathbf{k}}^{1,2}(r)$ since r is fixed.

By Lemma A.1,

$$(A.36) \quad \begin{aligned} \mathbb{E}[\hat{\omega} \hat{\mu}_i \hat{\mu}_j] &= \frac{1}{N N_r^2} \sum_{\mathbf{k} \in \mathcal{K}^{1,2}} B_{\mathbf{k}}^{1,2} \\ &= \frac{1}{N N_r^2} [N N_r^2 \mathbb{E}[\chi] \mathbb{E}[x_i] \mathbb{E}[x_j] + \mathcal{O}(N N_r + N_r^2)] \\ &= \mathbb{E}[\chi] \mathbb{E}[x_i] \mathbb{E}[x_j] + \mathcal{O}(N_r^{-1}) \\ &= \omega \mu_i \mu_j + \mathcal{O}(N_r^{-1}). \end{aligned}$$

Consider

$$(A.37) \quad \text{Var} [\hat{\omega} \hat{\mu}_i \hat{\mu}_j] = \mathbb{E} \left[(\hat{\omega} \hat{\mu}_i \hat{\mu}_j)^2 \right] - \mathbb{E} [\hat{\omega} \hat{\mu}_i \hat{\mu}_j]^2.$$

To compute $\mathbb{E} \left[(\hat{\omega} \hat{\mu}_i \hat{\mu}_j)^2 \right]$,

$$(A.38) \quad \begin{aligned} \mathbb{E} \left[(\hat{\omega} \hat{\mu}_i \hat{\mu}_j)^2 \right] &= \mathbb{E} \left[\left(\frac{1}{N} \sum_{k_1=1}^N \chi^{k_1} \right)^2 \left(\frac{1}{N_r} \sum_{k_2=1}^{N_r} x_i^{k_2} \right)^2 \left(\frac{1}{N_r} \sum_{k_3=1}^{N_r} x_j^{k_3} \right)^2 \right] \\ &= \frac{1}{N^2 N_r^4} \sum_{k_1, k_2=1}^N \sum_{k_3, k_4, k_5, k_6=1}^{N_r} \mathbb{E} \left[\chi^{k_1} \chi^{k_2} x_i^{k_3} x_i^{k_4} x_j^{k_5} x_j^{k_6} \right]. \end{aligned}$$

Using (A.1) and (A.2),

$$(A.39) \quad \mathbb{E} \left[(\hat{\omega} \hat{\mu}_i \hat{\mu}_j)^2 \right] = \frac{1}{N^2 N_r^4} \sum_{\mathbf{k} \in \mathcal{K}^{2,4}} B_{\mathbf{k}}^{2,4}.$$

By Lemma A.1,

$$(A.40) \quad \begin{aligned} \mathbb{E} \left[(\hat{\omega} \hat{\mu}_i \hat{\mu}_j)^2 \right] &= \frac{1}{N^2 N_r^4} \sum_{\mathbf{k} \in \mathcal{K}^{2,4}} B_{\mathbf{k}}^{2,4} \\ &= \frac{1}{N^2 N_r^4} \left[N^2 N_r^4 \mathbb{E} [\chi]^2 \mathbb{E} [x_i]^2 \mathbb{E} [x_j]^2 + \mathcal{O}(N^2 N_r^3 + N N_r^4) \right] \\ &= \mathbb{E} [\chi]^2 \mathbb{E} [x_i]^2 \mathbb{E} [x_j]^2 + \mathcal{O}(N_r^{-1}) \\ &= \omega^2 \mu_i^2 \mu_j^2 + \mathcal{O}(N_r^{-1}). \end{aligned}$$

Thus,

$$(A.41) \quad \begin{aligned} \text{Var} [\hat{\omega} \hat{\mu}_i \hat{\mu}_j] &= \mathbb{E} \left[(\hat{\omega} \hat{\mu}_i \hat{\mu}_j)^2 \right] - \mathbb{E} [\hat{\omega} \hat{\mu}_i \hat{\mu}_j]^2 \\ &= (\omega^2 \mu_i^2 \mu_j^2 + \mathcal{O}(N_r^{-1})) - (\omega \mu_i \mu_j + \mathcal{O}(N_r^{-1}))^2 \\ &= \mathcal{O}(N_r^{-1}). \end{aligned}$$

Since (A.36) and (A.41) hold for each $r = 1, \dots, R$,

$$(A.42) \quad \mathbb{E} \left[(\hat{C}_{\text{SIR}})_{ij} \right] = (C_{\text{SIR}})_{ij} + \mathcal{O}(N_{r_{\min}}^{-1}) \quad \text{and} \quad \text{Var} \left[(\hat{C}_{\text{SIR}})_{ij} \right] = \mathcal{O}(N_{r_{\min}}^{-1})$$

where $N_{r_{\min}}$ is the same from (4.12),

$$(A.43) \quad N_{r_{\min}} = \min_{1 \leq r \leq R} N_r.$$

The mean squared error for each element of \hat{C}_{SIR} is

$$(A.44) \quad \begin{aligned} \text{MSE} \left[(\hat{C}_{\text{SIR}})_{ij} \right] &= \text{Bias} \left[(\hat{C}_{\text{SIR}})_{ij} \right]^2 + \text{Var} \left[(\hat{C}_{\text{SIR}})_{ij} \right] \\ &= \left(\mathbb{E} \left[(\hat{C}_{\text{SIR}})_{ij} \right] - (C_{\text{SIR}})_{ij} \right)^2 + \text{Var} \left[(\hat{C}_{\text{SIR}})_{ij} \right] \\ &= \left((C_{\text{SIR}})_{ij} + \mathcal{O}(N_{r_{\min}}^{-1}) - (C_{\text{SIR}})_{ij} \right)^2 + \mathcal{O}(N_{r_{\min}}^{-1}) \\ &= \mathcal{O}(N_{r_{\min}}^{-1}). \end{aligned}$$

Next, we examine how the element-wise mean squared error in (A.44) translates to errors in the eigenvalue estimates. By Corollary 8.1.6 in [29],

$$(A.45) \quad \left| \lambda_k(\mathbf{C}_{\text{SIR}}) - \lambda_k(\hat{\mathbf{C}}_{\text{SIR}}) \right| \leq \|\mathbf{E}\|_2$$

where $\mathbf{E} = \mathbf{C}_{\text{SIR}} - \hat{\mathbf{C}}_{\text{SIR}}$. Since $\|\cdot\|_2 \leq \|\cdot\|_F$,

$$(A.46) \quad \left| \lambda_k(\mathbf{C}_{\text{SIR}}) - \lambda_k(\hat{\mathbf{C}}_{\text{SIR}}) \right| \leq \|\mathbf{E}\|_F.$$

Squaring both sides and taking the expectation,

$$(A.47) \quad \mathbb{E} \left[\left(\lambda_k(\mathbf{C}_{\text{SIR}}) - \lambda_k(\hat{\mathbf{C}}_{\text{SIR}}) \right)^2 \right] \leq \mathbb{E} [\|\mathbf{E}\|_F^2].$$

Consider

$$(A.48) \quad \mathbb{E} [\|\mathbf{E}\|_F^2] = \sum_{i,j=1}^m \mathbb{E} [E_{ij}^2] = \sum_{i,j=1}^m \mathbb{E} \left[\left((\mathbf{C}_{\text{SIR}})_{ij} - (\hat{\mathbf{C}}_{\text{SIR}})_{ij} \right)^2 \right] = \sum_{i,j=1}^m \text{MSE} \left[(\hat{\mathbf{C}}_{\text{SIR}})_{ij} \right].$$

By (A.44),

$$(A.49) \quad \mathbb{E} \left[\left(\lambda_k(\mathbf{C}_{\text{SIR}}) - \lambda_k(\hat{\mathbf{C}}_{\text{SIR}}) \right)^2 \right] = \mathcal{O}(N_{r_{\min}}^{-1})$$

as required. \square

A.4. Proof of Theorem 4.4.

THEOREM 4.4. *Assume the same conditions from Theorem 4.3. Then, for sufficiently large N ,*

$$(4.15) \quad \text{dist} \left(\text{colspan}(\mathbf{A}), \text{colspan}(\hat{\mathbf{A}}) \right) = \frac{1}{\lambda_n(\mathbf{C}_{\text{SIR}}) - \lambda_{n+1}(\mathbf{C}_{\text{SIR}})} \mathcal{O}_p(N_{r_{\min}}^{-1/2}).$$

Proof. Recall $\mathbf{A}, \hat{\mathbf{A}} \in \mathbb{R}^{m \times n}$ contain the first n eigenvectors of \mathbf{C}_{SIR} and $\hat{\mathbf{C}}_{\text{SIR}}$, respectively. Let $\mathbf{B}, \hat{\mathbf{B}} \in \mathbb{R}^{m \times (m-n)}$ contain the last $m-n$ eigenvectors of each matrix.

By Corollary 8.1.11 in [29], if

$$(A.50) \quad \|\mathbf{E}\|_2 \leq \frac{\lambda_n(\mathbf{C}_{\text{SIR}}) - \lambda_{n+1}(\mathbf{C}_{\text{SIR}})}{5},$$

then

$$(A.51) \quad \text{dist} \left(\text{colspan}(\mathbf{A}), \text{colspan}(\hat{\mathbf{A}}) \right) \leq \frac{4}{\lambda_n(\mathbf{C}_{\text{SIR}}) - \lambda_{n+1}(\mathbf{C}_{\text{SIR}})} \|\mathbf{E}_{21}\|_2$$

where $\mathbf{E} = \mathbf{C}_{\text{SIR}} - \hat{\mathbf{C}}_{\text{SIR}}$ and $\mathbf{E}_{21} = \mathbf{B}^\top \mathbf{E} \mathbf{A}$. In what follows, we show that (A.50) holds with high probability for sufficiently large N .

Theorem 2.6 from [51] states that for any $\tau > 0$

$$(A.52) \quad \mathbb{P} \left(\|\mathbf{E}\|_F \leq \tau \sqrt{\mathbb{E} [\|\mathbf{E}\|_F^2]} \right) \geq 1 - \frac{1}{\tau^2}.$$

Choose τ_* to be large such that $1/\tau_*^2$ is arbitrarily close to zero, and recognize that $N_{r_{\min}} \rightarrow \infty$ as $N \rightarrow \infty$ since $\omega(r) > 0$ for each $r = 1, \dots, R$. By (A.48), there exists N_* such that

$$(A.53) \quad \tau_* \sqrt{\mathbb{E}[\|\mathbf{E}\|_F^2]} \leq \frac{\lambda_n(\mathbf{C}_{\text{SIR}}) - \lambda_{n+1}(\mathbf{C}_{\text{SIR}})}{5}$$

when $N > N_*$. Combining this with (A.52),

$$(A.54) \quad \mathbb{P}\left(\|\mathbf{E}\|_F \leq \frac{\lambda_n(\mathbf{C}_{\text{SIR}}) - \lambda_{n+1}(\mathbf{C}_{\text{SIR}})}{5}\right) \geq 1 - \frac{1}{\tau_*^2}.$$

Since $\|\cdot\|_2 \leq \|\cdot\|_F$,

$$(A.55) \quad \mathbb{P}\left(\|\mathbf{E}\|_2 \leq \frac{\lambda_n(\mathbf{C}_{\text{SIR}}) - \lambda_{n+1}(\mathbf{C}_{\text{SIR}})}{5}\right) \geq 1 - \frac{1}{\tau_*^2}.$$

Thus, (A.50) is satisfied with probability $1 - 1/\tau_*^2$ when $N > N_*$. In this case,

$$(A.56) \quad \begin{aligned} \text{dist}\left(\text{colspan}(\mathbf{A}), \text{colspan}(\hat{\mathbf{A}})\right) &\leq \frac{4}{\lambda_n(\mathbf{C}_{\text{SIR}}) - \lambda_{n+1}(\mathbf{C}_{\text{SIR}})} \|\mathbf{E}_{21}\|_2 \\ &\leq \frac{4}{\lambda_n(\mathbf{C}_{\text{SIR}}) - \lambda_{n+1}(\mathbf{C}_{\text{SIR}})} \|\mathbf{E}\|_F \\ &\leq \frac{4}{\lambda_n(\mathbf{C}_{\text{SIR}}) - \lambda_{n+1}(\mathbf{C}_{\text{SIR}})} \tau_* \sqrt{\mathbb{E}[\|\mathbf{E}\|_F^2]}, \end{aligned}$$

by Corollary 8.1.11 in [29]. Thus,

$$(A.57) \quad \text{dist}\left(\text{colspan}(\mathbf{A}), \text{colspan}(\hat{\mathbf{A}})\right) = \frac{1}{\lambda_n(\mathbf{C}_{\text{SIR}}) - \lambda_{n+1}(\mathbf{C}_{\text{SIR}})} \mathcal{O}_p(N_{r_{\min}}^{-1/2}). \quad \square$$

A.5. Proof of Theorem 4.5.

THEOREM 4.5. *Let $f : \mathbb{R}^m \rightarrow \mathbb{R}$ with input probability measure $\pi_{\mathbf{x}}$ admit a central subspace $\mathcal{S}_{f, \pi_{\mathbf{x}}}$, and assume $\pi_{\mathbf{x}}$ admits an elliptically symmetric and standardized density function. Then, $\text{colspan}(\mathbf{C}_{\text{AVE}}) \subseteq \mathcal{S}_{f, \pi_{\mathbf{x}}}$.*

Proof. Consider the orthogonal $m \times m$ matrix $[\mathbf{A} \ \mathbf{B}]$ where $\mathbf{A} \in \mathbb{R}^{m \times n}$ and $\mathbf{B} \in \mathbb{R}^{m \times (m-n)}$ contain bases for $\mathcal{S}_{f, \pi_{\mathbf{x}}}$ and the orthogonal complement of $\mathcal{S}_{f, \pi_{\mathbf{x}}}$, respectively. Decompose \mathbf{x} into

$$(A.58) \quad \mathbf{x} = \mathbf{A}\mathbf{u} + \mathbf{B}\mathbf{v}$$

where $\mathbf{u} = \mathbf{A}^\top \mathbf{x} \in \mathbb{R}^n$ and $\mathbf{v} = \mathbf{B}^\top \mathbf{x} \in \mathbb{R}^{m-n}$.

Rewrite (4.17) as

$$(A.59) \quad \Sigma(y) = \int \mathbf{x} \mathbf{x}^\top d\pi_{\mathbf{x}|y}(\mathbf{x}) - \boldsymbol{\mu}(y) \boldsymbol{\mu}(y)^\top,$$

and decompose the first term of (A.59) similar to (A.23)

$$(A.60) \quad \int \mathbf{x} \mathbf{x}^\top d\pi_{\mathbf{x}|y}(\mathbf{x}) = \int \left[\int \mathbf{x} \mathbf{x}^\top d\pi_{\mathbf{x}|\mathbf{u}}(\mathbf{x}) \right] d\pi_{\mathbf{u}|y}(\mathbf{u}),$$

where $\pi_{\mathbf{x}|\mathbf{u}}$ and $\pi_{\mathbf{u}|y}$ are the conditional probability measures over $\mathcal{X}(\mathbf{u}) = \{\mathbf{x} \in \mathbb{R}^m : \mathbf{u} = \mathbf{A}^\top \mathbf{x}\}$ and $g^{-1}(y) = \{\mathbf{u} \in \mathbb{R}^n : g(\mathbf{u}) = y\}$, respectively. By (A.58),

$$(A.61) \quad \int \mathbf{x}\mathbf{x}^\top d\pi_{\mathbf{x}|\mathbf{u}}(\mathbf{x}) = \int (\mathbf{A}\mathbf{u} + \mathbf{B}\mathbf{v})(\mathbf{A}\mathbf{u} + \mathbf{B}\mathbf{v})^\top d\pi_{\mathbf{v}|\mathbf{u}}(\mathbf{v}),$$

where $\pi_{\mathbf{v}|\mathbf{u}}$ is the conditional measure induced by (A.58) and $\pi_{\mathbf{x}}$ over the set $\mathcal{X}(\mathbf{u})$ from (A.24). Expanding and simplifying (A.61),

$$(A.62) \quad \begin{aligned} \int \mathbf{x}\mathbf{x}^\top d\pi_{\mathbf{x}|\mathbf{u}}(\mathbf{x}) &= \int (\mathbf{A}\mathbf{u} + \mathbf{B}\mathbf{v})(\mathbf{A}\mathbf{u} + \mathbf{B}\mathbf{v})^\top d\pi_{\mathbf{v}|\mathbf{u}}(\mathbf{v}) \\ &= \int (\mathbf{A}\mathbf{u}\mathbf{u}^\top \mathbf{A}^\top + \mathbf{A}\mathbf{u}\mathbf{v}^\top \mathbf{B}^\top + \mathbf{B}\mathbf{v}\mathbf{u}^\top \mathbf{A}^\top + \mathbf{B}\mathbf{v}\mathbf{v}^\top \mathbf{B}^\top) d\pi_{\mathbf{v}|\mathbf{u}}(\mathbf{v}) \\ &= \mathbf{A}\mathbf{u}\mathbf{u}^\top \mathbf{A}^\top \left(\int d\pi_{\mathbf{v}|\mathbf{u}}(\mathbf{v}) \right) + \mathbf{A}\mathbf{u} \left(\int \mathbf{v}^\top d\pi_{\mathbf{v}|\mathbf{u}}(\mathbf{v}) \right) \mathbf{B}^\top \dots \\ &\quad + \mathbf{B} \left(\int \mathbf{v} d\pi_{\mathbf{v}|\mathbf{u}}(\mathbf{v}) \right) \mathbf{u}^\top \mathbf{A}^\top + \mathbf{B} \left(\int \mathbf{v}\mathbf{v}^\top d\pi_{\mathbf{v}|\mathbf{u}}(\mathbf{v}) \right) \mathbf{B}^\top \\ &= \mathbf{A}\mathbf{u}\mathbf{u}^\top \mathbf{A}^\top + \mathbf{B}\mathbf{B}^\top. \end{aligned}$$

Plugging this result into (A.60),

$$(A.63) \quad \begin{aligned} \int \mathbf{x}\mathbf{x}^\top d\pi_{\mathbf{x}|y}(\mathbf{x}) &= \int [\mathbf{A}\mathbf{u}\mathbf{u}^\top \mathbf{A}^\top + \mathbf{B}\mathbf{B}^\top] d\pi_{\mathbf{u}|y}(\mathbf{u}) \\ &= \mathbf{A} \left(\int \mathbf{u}\mathbf{u}^\top d\pi_{\mathbf{u}|y}(\mathbf{u}) \right) \mathbf{A}^\top + \mathbf{B}\mathbf{B}^\top. \end{aligned}$$

For $\mathbf{w} \in \text{null}(\mathbf{A}^\top)$,

$$(A.64) \quad \Sigma(y)\mathbf{w} = \left(\int \mathbf{x}\mathbf{x}^\top d\pi_{\mathbf{x}|y}(\mathbf{x}) \right) \mathbf{w} - \boldsymbol{\mu}(y)\boldsymbol{\mu}(y)^\top \mathbf{w} = \left(\int \mathbf{x}\mathbf{x}^\top d\pi_{\mathbf{x}|y}(\mathbf{x}) \right) \mathbf{w},$$

since $\boldsymbol{\mu}(y)^\top \mathbf{w} = 0$ as shown in (A.27). Therefore,

$$(A.65) \quad \begin{aligned} \Sigma(y)\mathbf{w} &= \left(\int \mathbf{x}\mathbf{x}^\top d\pi_{\mathbf{x}|y}(\mathbf{x}) \right) \mathbf{w} \\ &= \left(\mathbf{A} \left(\int \mathbf{u}\mathbf{u}^\top d\pi_{\mathbf{u}|y}(\mathbf{u}) \right) \mathbf{A}^\top + \mathbf{B}\mathbf{B}^\top \right) \mathbf{w} \\ &= \mathbf{A} \left(\int \mathbf{u}\mathbf{u}^\top d\pi_{\mathbf{u}|y}(\mathbf{u}) \right) (\mathbf{A}^\top \mathbf{w}) + \mathbf{B}\mathbf{B}^\top \mathbf{w} \\ &= \mathbf{0} + \mathbf{w} \\ &= \mathbf{w}. \end{aligned}$$

By (4.18), $\mathbf{w}^\top \mathbf{C}_{\text{AVE}} \mathbf{w} = 0$, which implies that $\mathbf{w} \in \text{null}(\mathbf{C}_{\text{AVE}})$. Therefore, $\text{null}(\mathbf{A}^\top) \subseteq \text{null}(\mathbf{C}_{\text{AVE}})$, which implies,

$$(A.66) \quad \text{colspan}(\mathbf{C}_{\text{AVE}}) \subseteq \text{colspan}(\mathbf{A}) = \mathcal{S}_{f, \pi_{\mathbf{x}}}$$

as required. \square

A.6. Proof of Theorem 4.6.

THEOREM 4.6. Assume that Algorithm 2.2 has been applied to the data set $\{[\mathbf{x}_i^\top, y_i]\}$, with $i = 1, \dots, N$, where the \mathbf{x}_i are drawn independently according to $\pi_{\mathbf{x}}$ and $y_i = f(\mathbf{x}_i)$ are point evaluations of f . Then, for $k = 1, \dots, m$,

$$(4.26) \quad \mathbb{E} \left[\left(\lambda_k(\mathbf{C}_{\text{SAVE}}) - \lambda_k(\hat{\mathbf{C}}_{\text{SAVE}}) \right)^2 \right] = \mathcal{O}(N_{r_{\min}}^{-1})$$

where $\lambda_k(\cdot)$ denotes the k th eigenvalue of the given matrix.

Proof. Algorithm 2.2 computes a sample approximation of (2.18),

$$(A.67) \quad \hat{\mathbf{C}}_{\text{SAVE}} = \sum_{r=1}^R \hat{\omega}(r) \left(\mathbf{I} - \hat{\Sigma}_h(r) \right)^2,$$

where

$$(A.68) \quad \hat{\omega}(r) = \frac{N_r}{N} \quad \text{and} \quad \hat{\Sigma}_h(r) = \frac{1}{N_r - 1} \sum_{i \in \mathcal{I}_r} (\mathbf{x}_i - \hat{\boldsymbol{\mu}}_h(r)) (\mathbf{x}_i - \hat{\boldsymbol{\mu}}_h(r))^\top$$

where \mathcal{I}_r is the set of indices such that $y_i \in J_r$, N_r is the cardinality of \mathcal{I}_r , and $\hat{\boldsymbol{\mu}}_h(r)$ is the sample estimate of the average from (2.12). Rewrite (A.68) as

$$(A.69) \quad \hat{\omega}(r) = \frac{1}{N} \sum_{i=1}^N \chi(y_i \in J_r) \quad \text{and} \quad \hat{\Sigma}_h(r) = \frac{1}{N_r - 1} \sum_{i \in \mathcal{I}_r} \mathbf{x}_i \mathbf{x}_i^\top - \frac{N_r}{N_r - 1} \hat{\boldsymbol{\mu}}_h(r) \hat{\boldsymbol{\mu}}_h(r)^\top$$

Fix r and let

$$(A.70) \quad \begin{aligned} \omega &= \omega(r), & \hat{\omega} &= \hat{\omega}(r), & \chi_i &= \chi(y_i \in J_r), \\ \boldsymbol{\mu} &= \boldsymbol{\mu}_h(r), & \hat{\boldsymbol{\mu}} &= \hat{\boldsymbol{\mu}}_h(r), & \boldsymbol{\Sigma} &= \boldsymbol{\Sigma}_h(r), & \text{and} & \hat{\boldsymbol{\Sigma}} &= \hat{\boldsymbol{\Sigma}}_h(r). \end{aligned}$$

Assume without loss of generality that $\mathcal{I}_r = \{1, \dots, N_r\}$.

To compute the mean squared error, we focus on the computation of a single element in $\hat{\mathbf{C}}_{\text{SAVE}}$. To do this, we move the sample index to the superscript and let the subscript denote the vector or matrix element similar to proof of Theorem 4.3.

Thus, for $1 \leq i, j \leq m$,

(A.71)

$$\begin{aligned}
 \mathbb{E} \left[\hat{\omega} \left(\delta_{ij} - \hat{\Sigma}_{ij} \right)^2 \right] &= \mathbb{E} \left[\left(\frac{1}{N} \sum_{k_1=1}^N \chi^{k_1} \right) \left(\delta_{ij} - \left(\frac{1}{N_r - 1} \sum_{k_2=1}^{N_r} x_i^{k_2} x_j^{k_2} \dots \right. \right. \right. \\
 &\quad \left. \left. \left. - \left(\frac{1}{N_r} \sum_{k_3=1}^{N_r} x_i^{k_3} \right) \left(\frac{1}{N_r} \sum_{k_4=1}^{N_r} x_j^{k_4} \right) \right) \right)^2 \right] \\
 &= \frac{\delta_{ij}}{N} \sum_{k_1=1}^N \mathbb{E} [\chi^{k_1}] - \frac{2\delta_{ij}}{N(N_r - 1)} \sum_{k_1=1}^N \sum_{k_2=1}^{N_r} \mathbb{E} [\chi^{k_1} x_i^{k_2} x_j^{k_2}] \dots \\
 &\quad + \frac{2\delta_{ij}}{NN_r^2} \sum_{k_1=1}^N \sum_{k_2, k_3=1}^{N_r} \mathbb{E} [\chi^{k_1} x_i^{k_2} x_j^{k_3}] \dots \\
 &\quad + \frac{1}{N(N_r - 1)^2} \sum_{k_1=1}^N \sum_{k_2, k_3=1}^{N_r} \mathbb{E} [\chi^{k_1} x_i^{k_2} x_j^{k_2} x_i^{k_3} x_j^{k_3}] \dots \\
 &\quad - \frac{2}{NN_r^2(N_r - 1)} \sum_{k_1=1}^N \sum_{k_2, k_3, k_4=1}^{N_r} \mathbb{E} [\chi^{k_1} x_i^{k_2} x_j^{k_2} x_i^{k_3} x_j^{k_4}] \dots \\
 &\quad + \frac{1}{NN_r^4} \sum_{k_1=1}^N \sum_{k_2, k_3, k_4, k_5=1}^{N_r} \mathbb{E} [\chi^{k_1} x_i^{k_2} x_j^{k_3} x_i^{k_4} x_j^{k_5}].
 \end{aligned}$$

Using (A.1) and (A.2)

$$\begin{aligned}
 \mathbb{E} \left[\hat{\omega} \left(\delta_{ij} - \hat{\Sigma}_{ij} \right)^2 \right] &= \frac{\delta_{ij}}{N} \sum_{k_1=1}^N \mathbb{E} [\chi^{k_1}] - \frac{2\delta_{ij}}{N(N_r - 1)} \sum_{\mathbf{k} \in \mathcal{K}^{1,1}} B_{\mathbf{k}}^{1,1} \dots \\
 \text{(A.72)} \quad &\quad + \frac{2\delta_{ij}}{NN_r^2} \sum_{\mathbf{k} \in \mathcal{K}^{1,2}} B_{\mathbf{k}}^{1,2} + \frac{1}{N(N_r - 1)^2} \sum_{\mathbf{k} \in \mathcal{K}^{1,2}} B_{\mathbf{k}}^{1,2} \dots \\
 &\quad - \frac{2}{NN_r^2(N_r - 1)} \sum_{\mathbf{k} \in \mathcal{K}^{1,3}} B_{\mathbf{k}}^{1,3} + \frac{1}{NN_r^4} \sum_{\mathbf{k} \in \mathcal{K}^{1,4}} B_{\mathbf{k}}^{1,4}.
 \end{aligned}$$

By Lemma A.1,

(A.73)

$$\begin{aligned}
\mathbb{E} \left[\hat{\omega} \left(\delta_{ij} - \hat{\Sigma}_{ij} \right)^2 \right] &= \frac{\delta_{ij}}{N} [N \mathbb{E} [\chi]] - \frac{2\delta_{ij}}{N(N_r - 1)} [NN_r \mathbb{E} [\chi] \mathbb{E} [x_i x_j] + \mathcal{O}(N + N_r)] \dots \\
&\quad + \frac{2\delta_{ij}}{NN_r^2} [NN_r^2 \mathbb{E} [\chi] \mathbb{E} [x_i] \mathbb{E} [x_j] + \mathcal{O}(NN_r + N_r^2)] \dots \\
&\quad + \frac{1}{N(N_r - 1)^2} [NN_r^2 \mathbb{E} [\chi] \mathbb{E} [x_i x_j]^2 + \mathcal{O}(NN_r + N_r^2)] \dots \\
&\quad - \frac{2}{NN_r^2(N_r - 1)} [NN_r^3 \mathbb{E} [\chi] \mathbb{E} [x_i x_j] \mathbb{E} [x_i] \mathbb{E} [x_j] + \mathcal{O}(NN_r^2 + N_r^3)] \dots \\
&\quad + \frac{1}{NN_r^4} [NN_r^4 \mathbb{E} [\chi] \mathbb{E} [x_i]^2 \mathbb{E} [x_j]^2 + \mathcal{O}(NN_r^3 + N_r^4)] \\
&= \delta_{ij} \mathbb{E} [\chi] - 2\delta_{ij} \mathbb{E} [\chi] \mathbb{E} [x_i x_j] + 2\delta_{ij} \mathbb{E} [\chi] \mathbb{E} [x_i] \mathbb{E} [x_j] \dots \\
&\quad + \mathbb{E} [\chi] \mathbb{E} [x_i x_j]^2 - 2 \mathbb{E} [\chi] \mathbb{E} [x_i x_j] \mathbb{E} [x_i] \mathbb{E} [x_j] \dots \\
&\quad + \mathbb{E} [\chi] \mathbb{E} [x_i]^2 \mathbb{E} [x_j]^2 + \mathcal{O}(N_r^{-1}) \\
&= \mathbb{E} [\chi] (\delta_{ij} - (\mathbb{E} [x_i x_j] - \mathbb{E} [x_i] \mathbb{E} [x_j]))^2 + \mathcal{O}(N_r^{-1}) \\
&= \omega \left(\delta_{ij} - \hat{\Sigma}_{ij} \right)^2 + \mathcal{O}(N_r^{-1}).
\end{aligned}$$

Consider

$$(A.74) \quad \text{Var} \left[\hat{\omega} \left(\delta_{ij} - \hat{\Sigma}_{ij} \right)^2 \right] = \mathbb{E} \left[\left(\hat{\omega} \left(\delta_{ij} - \hat{\Sigma}_{ij} \right)^2 \right)^2 \right] - \mathbb{E} \left[\hat{\omega} \left(\delta_{ij} - \hat{\Sigma}_{ij} \right)^2 \right]^2.$$

To find $\mathbb{E} \left[\left(\hat{\omega} \left(\delta_{ij} - \hat{\Sigma}_{ij} \right)^2 \right)^2 \right]$,

(A.75)

$$\begin{aligned}
\mathbb{E} \left[\left(\hat{\omega} \left(\delta_{ij} - \hat{\Sigma}_{ij} \right)^2 \right)^2 \right] &= \mathbb{E} \left[\left(\left(\frac{1}{N} \sum_{k_1=1}^N \chi^{k_1} \right)^2 \left(\delta_{ij} - \left(\frac{1}{N_r - 1} \sum_{k_2=1}^{N_r} x_i^{k_2} x_j^{k_2} \dots \right. \right. \right. \right. \\
&\quad \left. \left. \left. - \left(\frac{1}{N_r} \sum_{k_3=1}^{N_r} x_i^{k_3} \right) \left(\frac{1}{N_r} \sum_{k_4=1}^{N_r} x_j^{k_4} \right) \right) \right)^2 \right].
\end{aligned}$$

By expanding, we can rewrite (A.75) in a form which can be simplified using the tensor summation notation from (A.1) and (A.2). We then apply Lemma A.1 to simplify these summations and obtain

$$(A.76) \quad \mathbb{E} \left[\left(\hat{\omega} \left(\delta_{ij} - \hat{\Sigma}_{ij} \right)^2 \right)^2 \right] = \left(\omega \left(\delta_{ij} - \Sigma_{ij} \right)^2 \right)^2 + \mathcal{O}(N_r^{-1}).$$

Thus,

$$\begin{aligned}
 \text{Var} \left[\hat{\omega} \left(\delta_{ij} - \hat{\Sigma}_{ij} \right)^2 \right] &= \mathbb{E} \left[\left(\hat{\omega} \left(\delta_{ij} - \hat{\Sigma}_{ij} \right)^2 \right)^2 \right] - \mathbb{E} \left[\hat{\omega} \left(\delta_{ij} - \hat{\Sigma}_{ij} \right)^2 \right]^2 \\
 \text{(A.77)} \quad &= \left(\left(\omega \left(\delta_{ij} - \Sigma_{ij} \right)^2 \right)^2 + \mathcal{O}(N_r^{-1}) \right) \\
 &\quad - \left(\omega \left(\delta_{ij} - \Sigma_{ij} \right)^2 + \mathcal{O}(N_r^{-1}) \right)^2 \\
 &= \mathcal{O}(N_r^{-1}).
 \end{aligned}$$

Since (A.73) and (A.77) hold for each $r = 1, \dots, R$,

$$\text{(A.78)} \quad \mathbb{E} \left[(\hat{C}_{\text{SAVE}})_{ij} \right] = (C_{\text{SAVE}})_{ij} + \mathcal{O}(N_{r_{\min}}^{-1}), \quad \text{Var} \left[(\hat{C}_{\text{SAVE}})_{ij} \right] = \mathcal{O}(N_{r_{\min}}^{-1})$$

where $N_{r_{\min}}$ from (4.12) denotes the minimum number of samples in any one slice. From (A.78), the mean squared error for a single element of the SAVE matrix is

$$\text{(A.79)} \quad \text{MSE} \left[(\hat{C}_{\text{SAVE}})_{ij} \right] = \mathcal{O}(N_{r_{\min}}^{-1}).$$

Similar to the proof of Theorem 4.3, we use this mean squared error to obtain

$$\text{(A.80)} \quad \mathbb{E} \left[\|\mathbf{E}\|_F^2 \right] = \mathcal{O}(N_{r_{\min}}^{-1})$$

where $\mathbf{E} = \mathbf{C}_{\text{SAVE}} - \hat{\mathbf{C}}_{\text{SAVE}}$. Combining this result with Corollary 8.1.6 in [29] yields the desired result,

$$\text{(A.81)} \quad \mathbb{E} \left[\left(\lambda_k(\mathbf{C}_{\text{SAVE}}) - \lambda_k(\hat{\mathbf{C}}_{\text{SAVE}}) \right)^2 \right] = \mathcal{O}(N_{r_{\min}}^{-1}). \quad \square$$

A.7. Proof of Theorem 4.7.

THEOREM 4.7. *Assume the same conditions from Theorem 4.6. Then, for sufficiently large N ,*

$$\text{(4.27)} \quad \text{dist} \left(\text{colspan}(\mathbf{A}), \text{colspan}(\hat{\mathbf{A}}) \right) = \frac{1}{\lambda_n(\mathbf{C}_{\text{SAVE}}) - \lambda_{n+1}(\mathbf{C}_{\text{SAVE}})} \mathcal{O}_p(N_{r_{\min}}^{-1/2}).$$

Proof. In the proof of Theorem 4.6, we showed that

$$\text{(A.82)} \quad \mathbb{E} \left[\|\mathbf{E}\|_F^2 \right] = \mathcal{O}(N_{r_{\min}}^{-1})$$

where $\mathbf{E} = \mathbf{C}_{\text{SAVE}} - \hat{\mathbf{C}}_{\text{SAVE}}$. Given this result, the proof for Theorem 4.7 is identical to the proof for Theorem 4.4. \square

Acknowledgments. We thank Luis Tenorio and Don Estep for helpful discussions and insights regarding the work presented in this paper.

REFERENCES

- [1] S. ABBOTT, *Understanding Analysis*, Springer, New York, 2nd ed., 2001, <http://www.springer.com/us/book/9781493927111>.

- [2] K. P. ADRAGNI AND R. D. COOK, *Sufficient dimension reduction and prediction in regression*, Philosophical Transactions of the Royal Society of London A: Mathematical, Physical and Engineering Sciences, 367 (2009), pp. 4385–4405, <https://doi.org/10.1098/rsta.2009.0110>.
- [3] D. ALLAIRE AND K. WILLCOX, *Surrogate modeling for uncertainty assessment with application to aviation environmental system models*, AIAA Journal, 48 (2010), pp. 1791–1803, <https://doi.org/10.2514/1.J050247>.
- [4] P. CHALLENGOR, *Using emulators to estimate uncertainty in complex models*, in Uncertainty Quantification in Scientific Computing, A. M. Dienstfrey and R. F. Boisvert, eds., Berlin, Heidelberg, 2012, Springer Berlin Heidelberg, pp. 151–164, https://doi.org/10.1007/978-3-642-32677-6_10.
- [5] J. T. CHANG AND D. POLLARD, *Conditioning as disintegration*, Statistica Neerlandica, 51 (1997), pp. 287–317, <https://doi.org/10.1111/1467-9574.00056>.
- [6] A. COHEN, I. DAUBECHIES, R. DEVORE, G. KERKYACHARIAN, AND D. PICARD, *Capturing ridge functions in high dimensions from point queries*, Constructive Approximation, 35 (2012), pp. 225–243, <https://doi.org/10.1007/s00365-011-9147-6>.
- [7] P. G. CONSTANTINE, *Active Subspaces: Emerging Ideas for Dimension Reduction in Parameter Studies*, SIAM, Philadelphia, 2015, <http://doi.org/10.1137/1.9781611973860>.
- [8] P. G. CONSTANTINE, Z. DEL ROSARIO, AND G. IACCARINO, *Data-driven dimensional analysis: algorithms for unique and relevant dimensionless groups*, arXiv:1708.04303, (2017), <https://arxiv.org/abs/1708.04303>.
- [9] P. G. CONSTANTINE, A. EFTEKHARI, J. HOKANSON, AND R. WARD, *A near-stationary subspace for ridge approximation*, Computer Methods in Applied Mechanics and Engineering, 326 (2017), pp. 402–421, <https://doi.org/10.1016/j.cma.2017.07.038>.
- [10] P. G. CONSTANTINE, A. EFTEKHARI, AND M. B. WAKIN, *Computing active subspaces efficiently with gradient sketching*, in 2015 IEEE 6th International Workshop on Computational Advances in Multi-Sensor Adaptive Processing (CAMSAP), 2015, pp. 353–356, <http://doi.org/10.1109/CAMSAP.2015.7383809>.
- [11] R. D. COOK, *On the interpretation of regression plots*, Journal of the American Statistical Association, 89 (1994), pp. 177–189, <http://doi.org/10.1080/01621459.1994.10476459>.
- [12] R. D. COOK, *Using dimension-reduction subspaces to identify important inputs in models of physical systems*, in Proceedings of the Section on Physical and Engineering Sciences, American Statistical Association, Alexandria, VA, 1994, pp. 18–25, <http://users.stat.umn.edu/~rdcook/SDR/ASA94.pdf>.
- [13] R. D. COOK, *Graphics for regressions with a binary response*, Journal of the American Statistical Association, 91 (1996), pp. 983–992, <http://doi.org/10.1080/01621459.1996.10476968>.
- [14] R. D. COOK, *Regression Graphics: Ideas for Studying Regression through Graphics*, John Wiley & Sons, Inc, New York, 1998, <http://doi.org/10.1002/9780470316931>.
- [15] R. D. COOK, *SAVE: A method for dimension reduction and graphics in regression*, Communications in Statistics - Theory and Methods, 29 (2000), pp. 2109–2121, <http://doi.org/10.1080/03610920008832598>.
- [16] R. D. COOK AND L. FORZANI, *Likelihood-based sufficient dimension reduction*, Journal of the American Statistical Association, 104 (2009), pp. 197–208, <http://doi.org/10.1198/jasa.2009.0106>.
- [17] R. D. COOK AND S. WEISBERG, *Sliced inverse regression for dimension reduction: comment*, Journal of the American Statistical Association, 86 (1991), pp. 328–332, <http://www.jstor.org/stable/2290566>.
- [18] T. COWLING AND R. B. LINDSAY, *Magnetohydrodynamics*, Physics Today, 10 (1957), p. 40, <http://doi.org/10.1063/1.3060498>.
- [19] J. P. CUNNINGHAM AND Z. GHAHRAMANI, *Linear dimensionality reduction: Survey, insights, and generalizations*, Journal of Machine Learning Research, 16 (2015), pp. 2859–2900, <http://jmlr.org/papers/v16/cunningham15a.html>.
- [20] D. L. DONOHO, *High-dimensional data analysis: The curses and blessings of dimensionality*, in AMS Conference on Math Challenges of the 21st Century, 2000, <http://www-stat.stanford.edu/~donoho/Lectures/CBMS/Curses.pdf>.
- [21] M. L. EATON, *A characterization of spherical distributions*, Journal of Multivariate Analysis, 20 (1986), pp. 272–27, [http://doi.org/10.1016/0047-259X\(86\)90083-7](http://doi.org/10.1016/0047-259X(86)90083-7).
- [22] G. B. FOLLAND, *Real Analysis: Modern Techniques and Their Applications*, John Wiley & Sons Ltd, New York, 2nd ed., 1999, <https://www.wiley.com/en-us/Real+Analysis%3A+Modern+Techniques+and+Their+Applications%2C+2nd+Edition-p-9780471317166>.
- [23] M. FORNASIER, K. SCHNASS, AND J. VYBIRAL, *Learning functions of few arbitrary linear parameters in high dimensions*, Foundations of Computational Mathematics, 12 (2012), pp. 229–262, <http://doi.org/10.1007/s10208-012-9115-y>.

- [24] J. H. FRIEDMAN AND W. STUETZLE, *Projection pursuit regression*, Journal of the American Statistical Association, 76 (1980), pp. 817–823, <http://doi.org/10.1080/01621459.1981.10477729>.
- [25] K. FUKUMIZU AND C. LENG, *Gradient-based kernel dimension reduction for regression*, Journal of the American Statistical Association, 109 (2014), pp. 359–370, <https://doi.org/10.1080/01621459.2013.838167>.
- [26] R. GHANEM, D. HIGDON, AND H. OWHADI, *Handbook of Uncertainty Quantification*, Springer International Publishing, 2016, <http://doi.org/10.1007/978-3-319-11259-6>.
- [27] A. GLAWS AND P. G. CONSTANTINE, *Gauss–Christoffel quadrature for inverse regression: applications to computer experiments*, Statistics and Computing, (2018), <https://doi.org/10.1007/s11222-018-9816-4>.
- [28] A. GLAWS, P. G. CONSTANTINE, J. SHADID, AND T. M. WILDEY, *Dimension reduction in magnetohydrodynamics power generation models: dimensional analysis and active subspaces*, Statistical Analysis and Data Mining, 10 (2017), pp. 312–325, <http://doi.org/10.1002/sam.11355>.
- [29] G. H. GOLUB AND C. F. VAN LOAN, *Matrix Computations*, JHU Press, Baltimore, 4th ed., 2013, <https://jhupbooks.press.jhu.edu/content/matrix-computations>.
- [30] I. GOODFELLOW, Y. BENGIO, AND A. COURVILLE, *Deep Learning*, MIT Press, Cambridge, 2016, <http://www.deeplearningbook.org>.
- [31] T. HASTIE, R. TIBSHIRANI, AND J. FRIEDMAN, *The Elements of Statistical Learning: Data Mining, Inference, and Prediction*, Springer, New York, 2nd ed., 2009, <https://doi.org/10.1007/978-0-387-84858-7>.
- [32] J. HOKANSON AND P. CONSTANTINE, *Data-driven polynomial ridge approximation using variable projection*, arXiv:1702.05859, (2017), <https://arxiv.org/abs/1702.05859>.
- [33] M. E. JOHNSON, *Multivariate Statistical Simulation*, Wiley, Hoboken, 1987, <https://doi.org/10.1002/9781118150740>.
- [34] D. R. JONES, *A taxonomy of global optimization methods based on response surfaces*, Journal of Global Optimization, 21 (2001), pp. 345–383, <https://doi.org/10.1023/A:1012771025575>.
- [35] J. R. KOEHLER AND A. B. OWEN, *Computer experiments*, Handbook of Statistics, 13 (1996), pp. 261–308, [http://doi.org/10.1016/S0169-7161\(96\)13011-X](http://doi.org/10.1016/S0169-7161(96)13011-X).
- [36] J. A. LEE AND M. VERLEYSSEN, *Nonlinear Dimensionality Reduction*, Springer Science+Business Media, LLC, New York, 2007, <https://doi.org/10.1007/978-0-387-39351-3>.
- [37] K. C. LI, *Sliced inverse regression for dimension reduction*, Journal of the American Statistical Association, 86 (1991), pp. 316–327, <http://doi.org/10.1080/01621459.1991.10475035>.
- [38] K. C. LI, *On principal hessian directions for data visualization and dimension reduction: Another application of stein’s lemma*, Journal of the American Statistical Association, 87 (1992), pp. 1025–1039, <http://doi.org/10.1080/01621459.1992.10476258>.
- [39] K.-C. LI AND N. DUAN, *Regression analysis under link violation*, The Annals of Statistics, 17 (1989), pp. 1009–1052, <http://www.jstor.org/stable/2241708>.
- [40] W. LI, G. LIN, AND B. LI, *Inverse regression-based uncertainty quantification algorithms for high-dimensional models: theory and practice*, Journal of Computational Physics, 321 (2016), pp. 259–278, <http://doi.org/10.1016/j.jcp.2016.05.040>.
- [41] S. MUKHERJEE, Q. WU, AND D.-X. ZHOU, *Learning gradients on manifolds*, Bernoulli, 16 (2010), pp. 181–207, <https://doi.org/10.3150/09-BEJ206>.
- [42] R. H. MYERS AND D. C. MONTGOMERY, *Response Surface Methodology: Process and Product Optimization Using Designed Experiments*, John Wiley & Sons, New York, 1995.
- [43] Q. PAN AND D. DIAS, *Sliced inverse regression-based sparse polynomial chaos expansions for reliability analysis in high dimensions*, Reliability Engineering & System Safety, 167 (2017), pp. 484–493, <https://doi.org/10.1016/j.ress.2017.06.026>. Special Section: Applications of Probabilistic Graphical Models in Dependability, Diagnosis and Prognosis.
- [44] A. PINKUS, *Ridge Functions*, Cambridge University Press, 2015, <https://doi.org/10.1017/CBO9781316408124>.
- [45] M. M. RAO AND R. J. SWIFT, *Probability Theory with Applications*, Springer, New York, 2006, <https://doi.org/10.1007/0-387-27731-5>.
- [46] C. E. RASMUSSEN AND C. K. I. WILLIAMS, *Gaussian Processes for Machine Learning*, The MIT Press, Boston, 2006, <http://www.gaussianprocess.org/gpml/>.
- [47] S. RAZAVI, B. A. TOLSON, AND D. H. BURN, *Review of surrogate modeling in water resources*, Water Resources Research, 48 (2012), p. W07401, <https://doi.org/10.1029/2011WR011527>.
- [48] J. SACKS, W. J. WELCH, T. J. MITCHELL, AND H. P. WYNN, *Design and analysis of computer experiments*, Statistical Science, 4 (1989), pp. 409–423, <http://www.jstor.org/stable/2245858>.

- [49] T. J. SANTNER, B. J. WILLIAMS, AND W. I. NOTZ, *The Design and Analysis of Computer Experiments*, Springer Science+Business Media New York, 2003, <http://doi.org/10.1007/978-1-4757-3799-8>.
- [50] R. C. SMITH, *Uncertainty Quantification: Theory, Implementation, and Applications*, SIAM, Philadelphia, 2013, <http://bookstore.siam.org/cs12/>.
- [51] G. W. STEWART, *Stochastic perturbation theory*, SIAM Review, 4 (1990), pp. 579–610, <https://doi.org/10.1137/1032121>.
- [52] T. SULLIVAN, *Introduction to Uncertainty Quantification*, Springer, New York, 2015, <https://doi.org/10.1007/978-3-319-23395-6>.
- [53] J. F. TRAUB AND A. G. WERSCHULZ, *Complexity and Information*, Cambridge University Press, Cambridge, 1998.
- [54] H. TYAGI AND V. CEVHER, *Learning non-parametric basis independent models from point queries via low-rank methods*, Applied and Computational Harmonic Analysis, 37 (2014), pp. 389–412, <https://doi.org/10.1016/j.acha.2014.01.002>.
- [55] G. G. WANG AND S. SHAN, *Review of metamodeling techniques in support of engineering design optimization*, Journal of Mechanical Design, 129 (2006), pp. 370–380, <https://doi.org/10.1115/1.2429697>.
- [56] S. WEISBERG, *Applied Linear Regression*, John Wiley & Sons, Inc., New York, 3rd ed., 2005, <https://doi.org/https://doi.org/10.1002/0471704091>.
- [57] R. L. WHEEDEN AND A. ZYGMUND, *Measure and Integral: An Introduction to Real Analysis*, CRC, Boca Raton, 1977, <https://www.crcpress.com/Measure-and-Integral-An-Introduction-to-Real-Analysis-Second-Edition/Wheeden/p/book/9781498702898>.
- [58] Q. WU, J. GUINNEY, M. MAGGIONI, AND S. MUKHERJEE, *Learning gradients: Predictive models that infer geometry and statistical dependence*, Journal of Machine Learning Research, 11 (2010), pp. 2175–2198, <http://www.jmlr.org/papers/v11/wu10a.html>.
- [59] X. YIN, B. LI, AND R. D. COOK, *Successive direction extraction for estimating the central subspace in a multiple-index regression*, Journal of Multivariate Analysis, 99 (2008), pp. 1733–1757, <http://doi.org/10.1016/j.jmva.2008.01.006>.
- [60] J. ZHANG, W. LI, G. LIN, L. ZENG, AND L. WU, *Efficient evaluation of small failure probability in high-dimensional groundwater contaminant transport modeling via a two-stage Monte Carlo method*, Water Resources Research, 53 (2017), pp. 1948–1962, <https://doi.org/10.1002/2016WR019518>.